Scientific Research Publishing

Journal of Modern Physics, 2022, 13, 1530-1580
https://www.scirp.org/journal/jmp
ISSN Online: 2153-120X
ISSN Print: 2153-1196

Organizing and Disorganizing Resonances of Microtubules, Stem Cells, and Proteins Calculated by a Quantum Equation of Coherence

Hans J. H. Geesink[1], Marcus Schmieke[2,3]

[1]DSM-Research, Geleen, Netherlands
[2]Institute of Existential Consciousness Research (ECR), Berlin, Germany
[3]Dev Sanskriti University, Haridwar, India
Email: hans.geesink@ziggo.nl, Marcus.Schmieke@T-Online.de

How to cite this paper: Geesink, H.J.H. and Schmieke, M. (2022) Organizing and Disorganizing Resonances of Microtubules, Stem Cells, and Proteins Calculated by a Quantum Equation of Coherence. *Journal of Modern Physics*, **13**, 1530-1580.
https://doi.org/10.4236/jmp.2022.1312095

Received: October 13, 2022
Accepted: December 24, 2022
Published: December 27, 2022

Abstract

Conformational states of microtubules and proteins have typical spatial-spectral arrangements of atoms, called spatial coherence, that are characteristic for building, homeostasis, decay, and apoptosis. Microtubules show a principle of a self-organizing-synergetic structure called a Fröhlich-Bose-Einstein state. The spatial coherence of this state can be described by a toroidal quantum equation of coherence. In this space, microtubules and proteins have typical discrete frequency patterns. These frequencies comply with two proposed quantum wave equations of respective coherence (regulation) and decoherence (deregulation), that describe quantum entangled and disentangled states. The proposed equation of coherence shows the following typical scale invariant distribution of energy: $E_n = \hbar\omega_{ref} 2^q 3^m$. The proposed model supports quantum entanglement and is in line with the earlier published models of Fröhlich, Davydov, and Chern. A meta-analysis shows a semi-harmonic scale-invariant pattern for microtubules, stem cells, proteins, and EEG- and MEG-patterns. A fit has been found for about 50 different organizing frequencies and 5 disorganizing frequencies of measured microtubule frequencies that fit with the calculated values of the proposed quantum equations, which are positioned in a nested toroidal geometry. All measured and analysed frequencies of microtubules comply with the same energy distribution found for Bose-Einstein condensates. The overall results show a presence of an informational quantum code, a direct relation with the eigenfrequencies of microtubules, stem cells, DNA, and proteins, that supplies information to realize biological order in life cells and substantiates a collective Fröhlich-Bose-Einstein type of behaviour and further support the models of Tuszynski, Hameroff,

Bandyopadhyay, Del Giudice and Vitiello, Katona, Pettini, and Pokorny.

Keywords

Quantum Coherence, Coherence and Decoherence, Electromagnetic Frequencies, Quantum Biology, Quantum Wave Equation, Fröhlich, Microtubules, Proteins, Healthy and Unhealthy Frequency Patterns

1. Introduction Model of Fröhlich and Quantum Equations

Both classical and quantum electrodynamics predict the existence of dipole-dipole long-range electrodynamic intermolecular fields and can be observed and calculated. Various researchers have proposed the Fröhlich-Bose-Einstein principle for a self-organizing-synergetic structure, that works in biological processes and is also present in several systems of Boson-like quasi-particles in the condensed inorganic matter: Fröhlich [1], Davydov [2], Wu [3], Del Giudice, and Vitiello [4], Reimers [5], Chukova [6], Vasconcellos and Luzzi [7], Hameroff [8], Lundholm [9], Ahlberg Gagnér [10], De Ninno and Pregnolato [11], Nardecchia [12], Kadantsev [13], Scully [14], Hough and Hegmann *et al.* [15] [16], Wong [17], Zhedong Zhang [18], Pokorný and Vrba [19] [20], Geesink and Meijer [21] [22], Cui [23] and Khrennikov [24].

In 1968, Fröhlich showed that a driven set of oscillators of biological systems can condense with nearly all of the supplied energy activating the vibrational mode of the lowest frequency positioned, which is positioned in the band of THz (far infrared). A theory of coherent excitations at and above room temperature has been proposed, and attains a state of coherence, called a Fröhlich condensate [25] [26]. The supplied energy is not completely thermalized, but stored in a highly ordered fashion. This order expresses itself in long-range phase correlations and this phenomenon has a similarity with the vibrational states of Bose-Einstein condensates.

Geesink and Meijer substantiated Fröhlich's model and found a typical discrete semi-harmonic pattern of frequencies for biological systems as well as for Bose-Einstein condensates and elementary particles by analysing about 1200 biomedical and quantum physical publications, from 1970 till 2022. The biological systems showed either neutral or beneficial or detrimental biological effects related to internal and caused by external non-thermal electromagnetic signals at frequencies from ELF to THz and can be positioned at an invariant scale. It turned out that a Pythagorean-like equation can describe this distribution of energy: $E_n = \hbar\omega_{ref}2^q3^m$, which supports quantum entanglement, and that is in line with the earlier published models of Fröhlich, Davydov, Chern, and Chern-Simons. It is proposed that the model is a next step of the description of Fröhlich condensates and a high-temperature analogue of a Bose-Einstein condensate: the energy is not completely thermalized, used in maintaining coherent electromag-

netic wave processes, and can be positioned at an invariant scale of Chern numbers [27] [28].

The overall results show the presence of a molecular code-script, which supplies information to realize biological order in life cells and substantiates collective (Bose-Einstein) type of coherent wave behaviour. Based on this new biophysical principle, evidence is provided to support a causal relationship between exposure to electromagnetic waves and healthy or unhealthy effects on living cells and biomolecules. External exposures to non-thermal ELF, KHz, MHz and GHz, and THz electromagnetic waves with a decoherent (deregulating) nature can therefore lead to unhealthy conditions depending on wave frequency, pulsing properties, field intensity, and exposure time, whereas non-thermal ELF, KHz, MHz, GHz, and THz electromagnetic waves with a coherent lead to health conditions. Fröhlich regarded the high sensitivity of living cells to external waves with non-thermal Millimetre Waves (MMWs) in particular, as created by so-called resonance, representing one central feature of his theory [26]. He assumed, for example, that cancer induction pathways include a link with disturbed coherent electric vibrations. A cancer cell may escape from the essential interactions with the surrounding healthy cells and may exhibit an individual (independent) activity if the healthy frequency spectrum is perturbated [29]. Geesink and Meijer were able to prove this hypothesis by analysing about 120 biomedical studies related to cancer, showing a frequency band pattern of cancer-promoting and cancer-inhibiting frequencies that could be described by quantum wave interference and was explained by influences on the supposed Bose-Einstein type of cellular behaviour [21]. Biomolecules, living cells, and organisms obey to these similar informational frequency (energy) patterns, and follow typical eigenstate functions, that are differentiated by discrete coherent (regulating) and decoherent (deregulating) frequencies [20] [27] and see **Figure 1** and **Figure 2**.

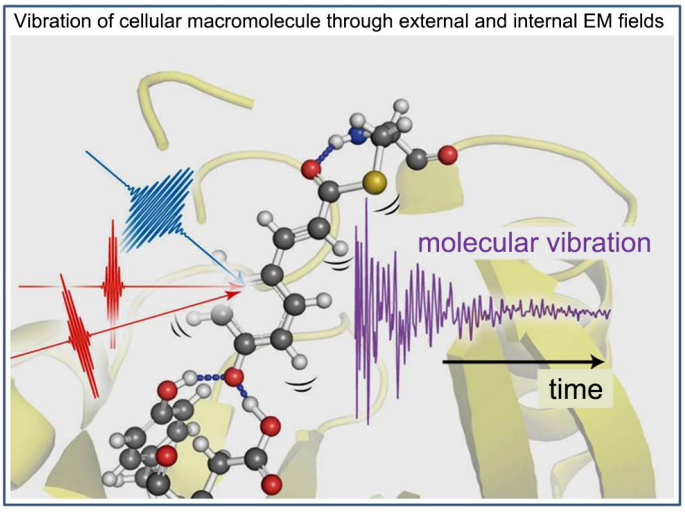

Figure 1. Internal (blue arrow) and external (red arrows) EM-fields with discrete wave frequencies influence the 3-D structure and vibratory states of macromolecules in life systems.

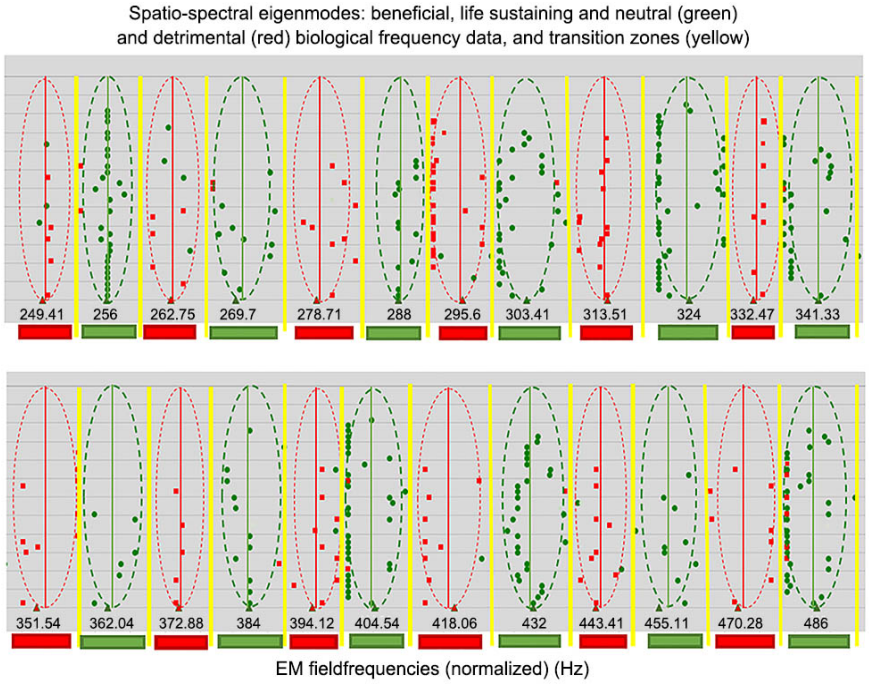

Figure 2. Measured/applied frequency data of living cells systems that are compatible with life conditions, or health-sustaining or health improving (coherent data and zones: green) and measured/applied frequency data of living cells systems that are detrimental for health (decoherent data: red) versus calculated normalized frequencies. Biological effects measured following exposures or endogenous effects of living cells *in vitro* and *in vivo* at frequencies in the bands of Hz, kHz, MHz, GHz, THz, PHz. Green triangles plotted on a logarithmic x-axis represent calculated normalized (Hz) health-sustaining frequencies; red triangles represent calculated health-destabilizing frequencies. Each point indicated in the graph is taken from published biological data and are a typical frequency for a biological experiment(s). For clarity, points are randomly distributed along the Y-axis; Yellow lines are transition frequencies (Geesink [28] [30]).

Hameroff and Tuszynski [8] proposed that the unitary oneness and inevitability of living systems suggest that higher-level quantum properties such as Bose-Einstein condensation, quantum coherent superposition, and entanglement are required to operate in biology to explain some of the more enigmatic features of life in general including consciousness. The typical characteristics of microtubules are an example of this statement.

Pokorný *et al.* [19] [20] proposed a mechanism for control, information and organization in biological systems, that is based on an internal coherent electromagnetic field. The electromagnetic field organizes and controls the motion and transport of molecules and their components, chemical reactions, information processes, communication inside and between cells, and many other activities. The electromagnetic field is supposed to be generated by microtubules composed of identical tubulin heterodimers with periodic organization and containing electric dipoles. A classical dipole theory has been used for the generation of the electromagnetic field to analyse space-time coherence. The structure of microtubules with helical and axial periodicity probably enables the interac-

tion of the field in time-shifted by one or more periods of oscillation and generation of coherent signals. Inner cavity excitation should provide equal energy distribution in a microtubule. The supplied energy coherently excites oscillators with a high electrical quality, microtubule inner cavity, and electrons at molecular orbitals and in "semiconduction" and "conduction" bands. The nonlinear properties of microtubules enable electromagnetic activity at lower and higher frequencies in the range from the acoustic to the UV region [19].

In this framework, a new quantum principle has been proposed and has been discussed in the context of the nature of brain processes and is called an equation of quantum entanglement: $E_n = \hbar\omega_{ref} 2^q 3^m$, or called a GM-scale by Meijer, or Geometric Musical Language (GML) by Bandyopadhyay, or General Music Code by Wong *et al.* [31] [32] [33]. The same type of principle has been proposed by Penrose and Hameroff and has been explained in the Orchestrated Objective Reduction Theory ("Orch") [8].

2. Coherence

Coherence is an ideal property of waves that enables stationary (*i.e.* temporally and spatially constant) interference. Coherence was originally conceived in connection with Thomas Young's double-slit experiment in optics but is now used in any field that involves waves, such as acoustics, electrical engineering, and quantum mechanics. Coherence has been defined as the physical congruence of wave properties within wave packets, and it is a property of stationary waves (*i.e.* temporally and spatially constant) that enables a type of wave interference, known as constructive. The processes are called coherent when the variability of the phase differences between the signals is relatively small, whereas the wave processes are defined as incoherent, the phase difference has a high degree of variability. A relation has also been found between self-similarity and squeezed coherent states that are so-called deterministic fractals. Fractal properties are incorporated into the framework of the theory of analytical functions and coherent states [34].

Space coherence in life processes

The microtubules of the cytoskeleton are example of biological entities, which depend on the coherent properties of the underlying intra- and extra-cellular water [35]. Electric polarization waves predicted by Fröhlich in living cells, Boson condensation, are identified as the Goldstone massless modes which appear as a consequence of the spontaneous breakdown of the SU(2) dipole-otational symmetry. This breaking is provided by the water polarization induced by Davydov solitons travelling on molecular chains [4]. The ability of water within living matter to display macroscopic quantum-properties as long-range correlations and the described structures is based on complex Bose-Einstein condensations of its dipole-wave-quanta in the quantum vacuum. The underlying dynamical processes of these fractal and self-similar structures are infinite iterative as shown by the mathematics of self-similar fractals according to Vitiello [36]. The resulting macroscopic coherent quantum-objects as microtubules and co-

herent domains of water connect the outer realm with the inner realm of life as a unit of meaningful information. The outer realm of life can be described as consisting of classically separated entities like atoms and molecules whereas the inner dimension of life consists of entities of undividable wholeness. The transition from outer fragmentation to inner wholeness can be described by a four valued logical system, which includes an infinite iterative process as its third value and by spatial coherence [28] [37]. The classical Aristotelian logic reaches its limitation in describing the life process, as it can distinguish objective matter from subjective consciousness and fails to understand the interaction between both and the intermediate realm of mixed subjectivity which escapes as the tertium non datur [38].

In this table, the four valued logical structure is expressed in 4 levels of reflection starting with the water-molecules and its waves, which are the 0th level of reflection as irreflexive matter [39] and see **Table 1**. The dipole-wave-quanta are the first level of reflexion, expressing an order of the water-waves on the level of a higher wholeness. The second level of reflexion can be iterated infinitively and in this way is creating the spatial coherent structure of the Bose-Einstein-condensate characterized by a fractal self-similar structure and to be described by space information [28]. The final third level of reflection corresponds to the information contained in this informative state in the quantum-vacuum, see **Figure 3** and **Figure 4**. This is especially significant for microtubules as according to the theory of Hameroff and Penrose orchestrated reduction of the wave function within the intercellular network of microtubules, that is a candidate for the physical correlate of consciousness [40].

Table 1. 4 values of the life process up to the quantum-vacuum.

Level of reflection	Structure
0	1 Water dipole-molecules
1	2 Dipole-wave-quanta
2	3 Bose-Einstein-condensate wave quanta
3	4 Integrated information state of quantum-vacuum

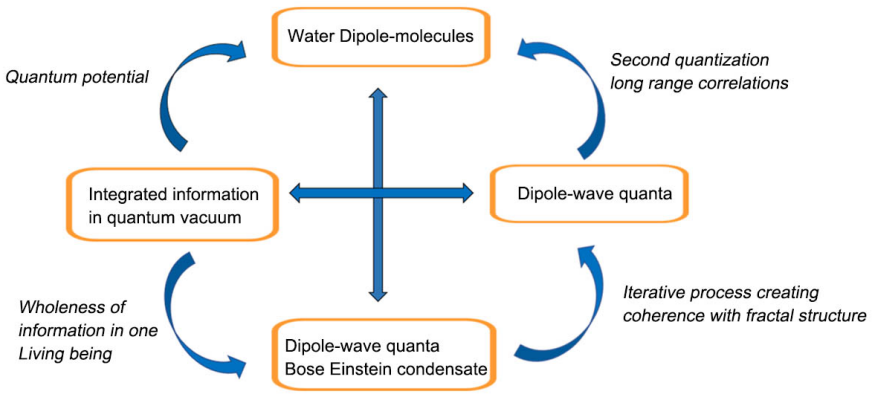

Figure 3. Threefold reflections from Bose-Einstein condensate to quantized information.

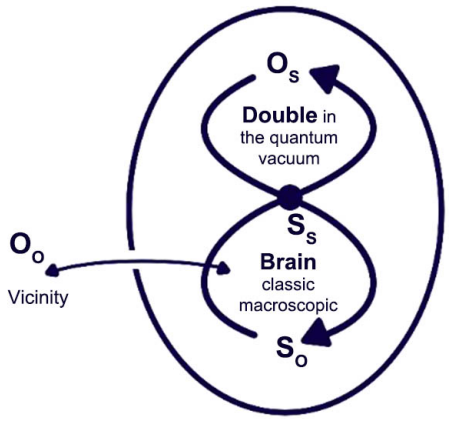

Figure 4. Four valued structures of the brain-double-consciousness-environment ensemble.

The fourth value is created by a final reflection on the total self-similar fractal coherent process itself. In this way, the infinite iterative processes underlying macroscopic coherence are the intermediate area between outside and inside which characterize life itself and give rise to consciousness [41]. Self-consciousness is a property of living entities and can be described by a four valued system of self-reflecting processes within the quantum-structure of the brain and its double in the quantum vacuum according to Vitiello. These four valued formalisms contain next to the pure states of Aristotelian logic S_S and O_O the mixed states of S_O and O_S, which correspond to the tertium non datur of two valued logics. In this way the subject-object gap is overcome by a dynamical four-valued process which creates a subjectively objective realm between the subject of consciousness and its material counterpart. The resulting coherent dynamics can be for example made visible in the appearance of coherent domains in the water of the brain, the coherent structures constituting the microtubules and coherent behaviour of the neuronal signals visible in the EEG [31] [32] [33] [42].

A meta-analysis by Geesink and Meijer demonstrated that frequency patterns of biomolecules including brain waves in normal healthy cells are positioned at the coherent pointer state frequencies of the proposed quantum equation. In contrast, biomolecules present in diseased cells of deregulated brain waves are positioned at typical decoherent frequency patterns. Based on these results an integral biological model has been inferred that makes use of four types of attractors: static fixed-point frequencies; a periodic repetition of sequences of twelve basic reference intervals; a periodic torus geometry; and a chaos attractor positioned just in between coherent pointer states related to decoherence. Quantum decoherence is the loss of quantum coherence, and decoherence can be viewed as the loss of information from a system into the environment (often modelled as a heat bath), since every system is loosely coupled with the energetic state of its surroundings [43].

It was Schrödinger who recognized that coherent interaction of waves is coupled to entanglement as "the characteristic aspect of quantum mechanics"

and suggested that "eigenstates" can survive interaction with the environment. In quantum mechanics, all objects have wave-like properties (see de Broglie waves). Also, discrete brain frequencies including patterns measured by EEG and MEG fit in a coherent or in a decoherent frequency pattern and can be substantiated by a quantum physical model about phase-synchronisation. The spatio-spectral eigenmodes are related to a discrete toroidal distribution of energy: $E_n = \hbar\omega_{ref} 2^q 3^m$. Healthy states are quantum coherent and approach a global quantum coherence of 1.0, while unhealthy states are decoherent and cause a decrease of coherence. The proposed model of spatio-spectral eigenmodes has been substantiated by analysing the many measured frequency patterns of EEG's and MEG's, and electromagnetic exposures of brain cells, microtubules, glands, and neurons [44]. Geesink and Meijer found further support for the Fröhlich condensation not only for the long-range electromagnetic waves but also for shorter and much longer waves in a meta-analysis of endogenous and exogenous electromagnetic waves for living cells and biomolecules. Unique wave frequency patterns have been found in two meta-analyses of about 750 published articles of biological electromagnetic experiments, in which spectra of biomolecules and exposures to non-thermal electromagnetic waves have been analysed [21] [45]. It turns out that biological systems show a clear spectral scale invariant coherence. A similar meta-analysis of Einstein-Podolsky-Rosen (EPR) and Bose-Einstein condensates learned that entanglement, achieved in the experiments is real, and that applied EMF-frequencies are again located at discrete coherent configurations. Strikingly, all analysed EPR-data and BEC's of the independent studies fit precisely in the inferred scale of coherent frequency bands or called spatial coherence and turned out to be virtually congruent with a semi-harmonic frequency-scale for living organisms [46] [47]. A quantum equation of a coherent entangled distribution of energy (3D semi-harmonic oscillator) has been derived, that is in line with the earlier published models of Fröhlich and Davydov [1] [2] [26] [48] [49].

1) Quantum wave equation of an entangled energy state E_n:

$$E_n = \hbar\omega_{ref} 2^q 3^m$$

E_n: Energy coherent state n (n = 1 till > 12 × 52); $\hbar$: Reduced Planck's constant, frequency. ω_{ref}: 1 Hz, $q = n + p$; n: series of numbers: 0, 0.5, 2, 4, 5, 7, 8, −1, −3, −4, −6, −7; p: series of numbers: <−4, −4, −3, −2, −1, 0, 1, 2, 3, 4, 5, 6, >52; m: series of numbers: 0, 1, 2, 3, 4, 5, −1, −2, −3, −4, −5.

2) Quantum equation of a disentangled energy state E_x, of which these states are logarithmically just positioned in between the different coherent states:

$$E_x = 10^{0.5\log E_n + 0.5\log E_{n+1}}$$

E_x: Energy decoherent state x (x = 1 till > 624); E_n: Energy coherent state n (n = 1 till > 624).

3) Quantum wave equation of the sum of entangled energy states E_n:

$$E_{n,sum} = \sum_i \hbar\omega_{ref} 2^q 3^m$$

$E_{n,sum}$ is the total amount of involved (i)-energy states; the amount of the states (i) is still unknown, but probably > 624, based on physical experiments.

The distributed energies are described by ratios of 1:2, or 2:3 and close approaches thereof, and are a small adaptation of Pythagorean tuning, and make use of standing waves in a toroidal Riemannian Tonnetz geometry and valued weightings of 12 fundamental frequencies. The same model could be applied for the measured energy distributions of BEC's, superconductors and EPR-experiments [46]. The detected eigenfrequencies are arithmetically scaled according to a semi-harmonic scale and exhibit a core pattern of twelve eigenfrequency functions with adjacent self-similar patterns, according to octave hierarchy [22] [45]. The proposed quantum wave equation of coherence can be analytically calculated by the normalisation of Chern numbers, which are the 12 basic elements of the proposed quantum wave equation of coherence and calculated by the partial flag manifolds Fn. The Chern numbers are the determinants of the quantum metric and topological invariants and have calculated in the period of 1950-2022 [28] and see **Figure 5**. Interestingly a same type of model of nested tori has been calculated by Amiot [50] for the tori of phases for musical scales. For example: the circle of "fifths" can be positioned at rotoids (composed motions of rotations), that circles or spiralizes each sub-unit of the nested tori, together with inscribed triads, major-third, and minor-third relations, see **Figure 6**.

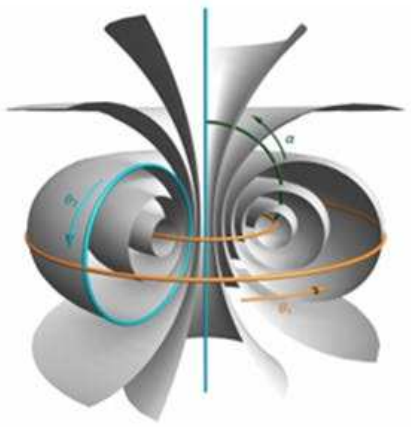

Figure 5. Toroidal geometry (reference: Balch *et al.*, 2020).

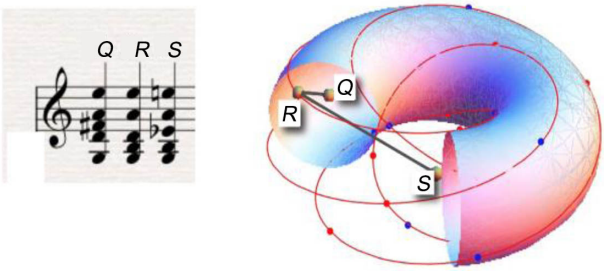

Figure 6. An acoustic model: Angular distances between complex chords (reference: Amiot, 2013).

A next step of the extension of the Fröhlich model may be based on this meta-analysis of about 1200 data of living cells/molecules and inanimate entangled quantum process: Conformational states of living cells/molecules have typical spatial arrangements of atoms, which are characteristic for building, homeostasis, decay and apoptosis. In quantum physics, complementary non-interchangeable observables such as location can be related to a wave function in the complex number space. In this space, all living cells/molecules are located, that show discrete frequency or called energy positions at a proposed toroidal space, described by quantum wave equation of coherence (regulation) or decoherence (deregulation). Within this toroidal space, microtubules are organized.

A same scale invariant principle can be found for microtubules, whereas microtubules mediate between the control centre (the centriole) and the autonomous domains. The control centre detects objects and other cells by pulsating near infrared signals among other frequency bands. In response to external electromagnetic signals, the centrosome is expected to send destabilizing signals along the array of microtubules radially emanating from it. The signal is then transduced into an electromagnetic wave that can propagate along the microtubules like action potentials along nerves [8]. The centrosome as the main microtubule organization centre is composed of a centriole pair surrounded by Pericentriolar Material (PCM). Interphase PCM components adopt a concentric toroidal distribution of discrete diameter around centrioles [51]. A mechanistic model for centrosome function has already been developed during mitosis, in which centrosome functions as an electronic generator. In particular, the spinal rotations of centrioles transform the cellular chemical energy into cellular electromagnetic energy. This explains the self-organized orthogonal configuration of the two centrioles in a centrosome, which is through the dynamic electromagnetic interactions of both centrioles of the centrosome [52]. Microtubules and motors proteins have been investigated, that is populated by a high density of defects—tiny regions where the local alignment is lost. The biochemical activity provided by the kinesin motors brings the defects to life, moving them around like swimming microorganisms and exploring the toroidal space [53].

The registered frequencies of brain waves as well as microtubules obey to the frequency patterns described by the proposed toroidal equation of coherence and located at a toroidal geometry. Molecules positioned at this toroidal space show a healthy state (regulation), or positioned at a state in-between, that are unhealthy states and show predominantly decoherent states (deregulation). Healthy states are quantum entangled states, whereas unhealthy states are the disentangled states. Therefore, it is considered that the toroidal organisation of microtubules is possible by an intermittent pattern of coherent organisation intertwined with a coherent and decoherent organisation of biomolecules. This intermittent pattern has been found for a nematic order on curved surfaces and is often disrupted by the presence of topological defects, which are singular regions in which the orientational order is undefined, defects in the otherwise aligned ma-

terial [52] and see **Figure 7**. It is proposed that the electromagnetic fields generated by synchronized oscillation of microtubules, centrosomes, and chromatin fibres facilitate the several events during mitosis and meiosis, including centrosome trafficking, chromosome congression in mitosis and synapsis between homologous chromosomes in meiosis. These intracellular electromagnetic fields are generated under energy excitation through the synchronized electromagnetic oscillations of the dipolar structures [54].

Analysis of the different studies of measured frequencies of microtubules learns that the frequencies of these waves are just positioned at the pointer states of the proposed toroidal quantum wave equation of coherence and are located at a toroidal geometry, see later.

3. Electromagnetic Fields and Biomolecules

Polarization is an ordering in space of electrical charges and waves in response to an external alternating electric field, and application of an electromagnetic field to a dielectric, such as biomatter, leads to different types of polarization mechanisms: ionic, interfacial dipolar, atomic and electronic polarizations. There is an order of polarization and relaxation mechanisms have been observed when an alternating electric field of increasing frequency is applied to biological matter: ionic diffusion is observed at low frequencies, followed by interfacial and dipolar relaxation, followed by atomic and electronic resonances at much higher frequencies (see **Figure 8** and **Figure 9**).

The biological components of living cells, including the solutes dissolved in water, all have their typical resonances and spectra, which respond to electromagnetic fields. The dipole relaxation, ionic, atomic and electron polarization, and such features in the whole cell are ordered according to their resonant frequencies. Endogenous electromagnetic fields are self-generated by internal vibrations of living cells and their constituents play an important role in biological self-organization. On the other hand, external electromagnetic fields at sub-thermal intensities can influence the intrinsic endogenous electromagnetic fields and can have an impact on conformational states and self-organisation of biomolecules [45] [55] [56] [57].

The physical basis for the interaction between biological systems and Electromagnetic (EM) fields rest, in part, on the separate dielectric and spectroscopic properties of the molecular constituents and aggregates that comprise the biological system. For example, the millimetre wave and far-infrared spectrum show contributions due to intermolecular vibrations involving clusters of H_2O molecules and it is recognized that hydrogen bonded interactions with biomolecules occur. The role of structural H_2O is closely tied to the dynamics of the phase transitions of biopolymers, which are known to be cooperative. Terahertz interactions with biological matter, ranging from simple molecules like water, ionized salts, and nitric oxide, to complex biopolymers such as DNA, sugars, and proteins, and to cells and whole tissues play a role [57].

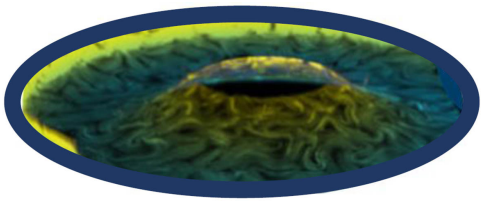

Figure 7. Imagine of a tiny donut-shaped droplet, covered with wriggling worms, with bundles of rod-like microtubules forming the filaments, kinesin motor proteins acting as the engines, and ATP as the fuel (reference: Ellis *et al*., 2017 and the analogy with intertwining of coherence and decoherent zones).

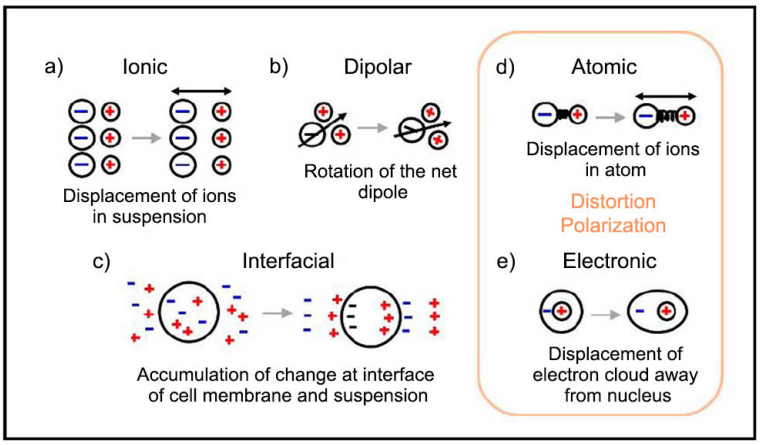

Figure 8. Application of an electromagnetic field to a dielectric, such as biomatter, leads to different types of polarization mechanisms: ionic, interfacial dipolar, atomic, and electronic polarizations, reference Mehrota according to Geesink [30].

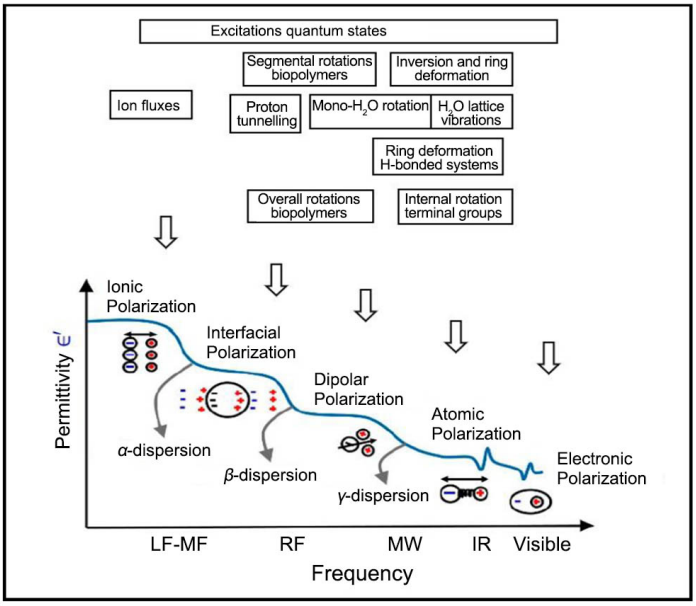

Figure 9. The order of polarization and relaxation mechanisms observed when an alternating electromagnetic field of increasing frequency is applied to biological matter. Ionic diffusion is observed first, followed by interfacial and dipolar relaxations, followed by atomic and electronic resonances reference Mehrota according to Geesink [30].

Also, external non-thermal electromagnetic waves play a role involving secondary and tertiary structures of biopolymers by processes involving the initial uptake of EM energy by structural H_2O, an analogous possibility exists for the intervention into the structure of for example membranes. Apart from the effect of the degree of cooperativity in these phase transitions (biopolymer or biological membrane), it is expected that any external EM-field effects will be maximal under thermodynamic and chemical conditions close to the phase-transition point. Biochemically actuated conformational changes *in vivo* systems will affect the status of the (cooperative) phase transitions, and hence the susceptibility of the associated conformations to energy uptake including by structural H_2O [58] [59] [60] and see **Figure 9**.

According to Illinger: "If the absorption and emission of electromagnetic waves from a system containing a set of vibrational modes k, is associated with a coherent non-linear, coupled electromagnetic transitions, an excitation of the lowest mode analogous to a Bose-condensation results. Such excitations would have consequences for the establishment of selective interactions among the chemical species partaking of biochemical processes and the influences of external man-made on vibrational modes [1] [48] [59] [60]. In the presence of pumping, of energy S_k, from the thermal bath into the modes k, a Planck-type distribution of photons over the modes k, and hence a Boltzmann-type distribution of molecular systems over vibrational states (ν_1, ν_2, …, ν_j, …, ν_k, …, ν_z) results from linear systems. In contrast, for a non-linear Fröhlich system, the distribution differs in a salient fashion from the modified Planck distribution and the Debye model. The Debye model estimates the phonon contribution to the specific heat in a solid and treats the vibrations of the atomic lattice (heat) as phonons in a box, in contrast to the Einstein model, which treats the solid as many individuals, non-interacting quantum harmonic oscillators".

"This condensation into the lowest-frequency state has been proposed equivalent to the Bose condensation, and μ, of the mentioned equation plays a role analogous to the chemical potential in the Einstein condensation of a Bose-Einstein gas. It is expected that dissipative biological structures that are linked by a set of biochemical reactions and physical conformational states, and characterized by chemically pumped steady states, connected by non-reactive collisions, exhibit the non-linear behaviour of coupled photon exchange processes requisite for the Bose-condensation [30] [59] [60]. According to Illinger: "Energy absorption from an external EM field coupling to an equilibrium system, and hence closely related to a bulk attenuation function, $\alpha(\omega)$, is not expected to show frequency-selective effects of a pronounced sort, since the bulk attenuation function of ordinary aqueous dielectrics is not expected per se to show such features. But the excitation of a Bose-type condensation as predicted by Fröhlich, and the existence of dissipative structures in the more general sense provide for the possibility of these effects. Such interactions manifest themselves in a quasi-resonant, frequency-selective (interaction with a global biological endpoint, e.g. cell

growth rate, if the dynamical variables of linked organisation patterns as well as biochemical reactions couple with an external EM field. Although such effects are possible even with systems involving very simple molecular species, one may speculate that, in the case of certain types of biochemical systems, which involve, among other interactions, conformational changes in biopolymers during the chemical reaction, the frequency regime for such effects lie in the millimetre-wave and far-infrared region [59]", but are according to Geesink also coupled to much lower and higher coherent frequencies [30] and see **Figure 10**.

In fact, Fröhlich has suggested that, owing to the possibility that evolutionary processes have played a dominant role in selecting the molecular systems which show the Bose-condensation, vibrations connected with that mechanism may be pervasive in many types of biological tissue, not only simple cellular entities. In general, direct photon and phonon spectroscopic determinations of millimetre-wave and far-infrared properties of *in vivo* biological systems possess the considerable advantage of providing biophysical information at the molecular-systems level, while global biological endpoints (e.g. cell growth rate) are, by their very nature, integrative effects. In this sense, the frequency range predicted for the biomolecules and quasi-lattice vibrations of the biopolymers, of about sub-Hertz to PHz are proposed to be scale invariant and may be thought of as the frequency regime in which EM-field interactions with the dissipative system are most likely to occur [22] [29] [59] [60].

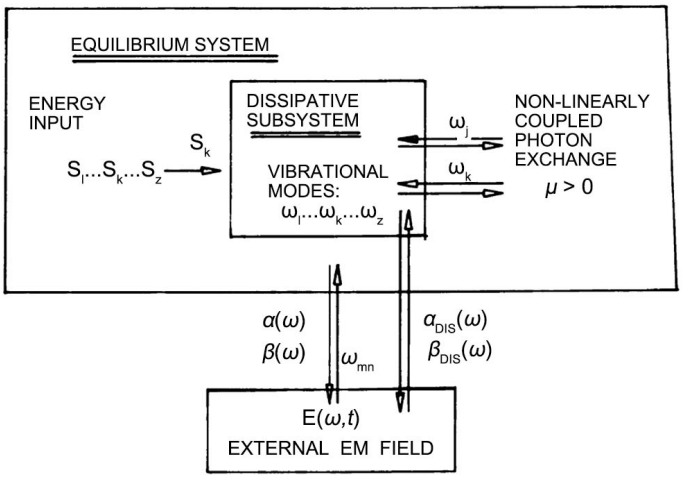

Figure 10. Formal representation of the interaction of an external EM field with the dissipative subsystem in the Fröhlich vibrational model (μ is the nonlinear coupling parameter of the proposed Fröhlich/Illinger equation); Vibrational states and representative photon-induced transitions for the set of vibrations ω_1, ω_2, …, ω_k, …, ω_z in the Frohlich vibrational model. v_k is the vibrational quantum number of the k'th mode, ω_k its frequency, and S_k the rate of the (pumped) energy transfer into the modes k of the dissipative subsystem by the surroundings. $\alpha(\omega)$ and $\beta(\omega)$ are the attenuation function and the biological-response function for the equilibrium system; $\alpha_{DIS}(\omega)$and $\beta_{DIS}(\omega)$are the same functions, respectively, for the dissipative subsystem; ω is the frequency of the EM field (reference: Illinger, 1981).

4. Topology Electromagnetic Regulation of Biomolecules

4.1. Collective Entangled Electromagnetic Oscillations of Microtubules

The fundamental significance of the electromagnetic field in biological functions corresponds also to the loci of its generation—the central part of cells with microtubules is also devoted to this procedure. Microtubules (MTs), the main components of cytoskeleton, are the structures conditioning the existence and structure of multicellular organisms. The MTs are self-assembled linear hollow circular tubes with inner and outer diameters of 17 and 25 nm and filed with water molecules, respectively, growing from the centrosome of the cell towards its membrane and forming a radial system and see Figures 11-13.

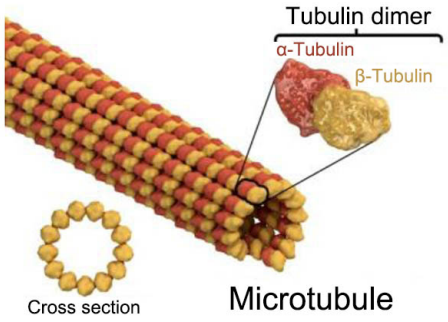

Figure 11. Microtubule (reference: Biology Dictionary).

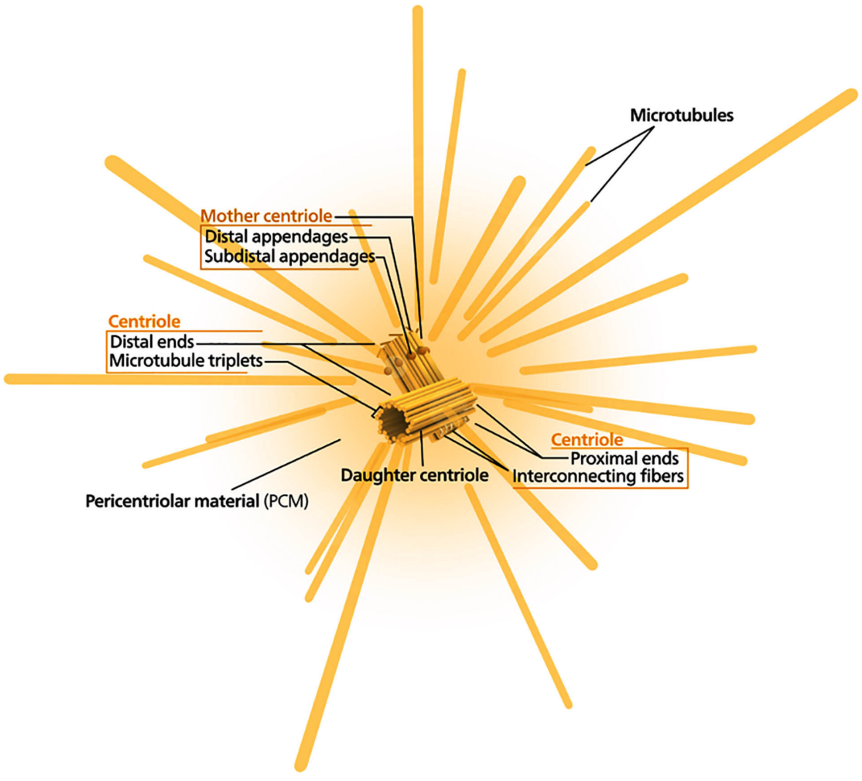

Figure 12. The structure of the centrosome (Wikipedia, centrosome).

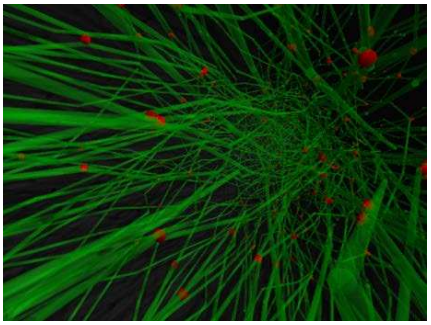

Figure 13. Inside view of a network of microtubule inside the axon of a neuron. Red blobs represent linker proteins that attach two microtubules together at a point (reference: Nikolov and Shah, 2009).

They are polymers built of tubulin heterodimers with a helical periodicity of 13 heterodimers along a helix turn. A tubulin heterodimer consists of two subunits: alfa and beta tubulin and spindle fibres form a protein structure that divides the genetic material in a cell. They provide many activities such as material transport, cell motility, division, etc. and the centrosome is an organelle that serves as the main microtubule organizing centre of the human cell, as well as a regulator of cell-cycle progression [61]. The three elements: microtubules, cytoskeleton, and its components—actin, and intermediate filaments are engaged in an extensive crosstalk that is important for core biological processes. Actin-microtubule crosstalk is particularly important for the regulation of cell shape and polarity during cell migration and division and the establishment of neuronal and epithelial cell shape and function [62]. MTs are also considered as bio-electrochemical transistors that form nonlinear electrical transmission lines [63]. Very likely, microtubules facilitate information processing [19] [64] [65] whereas hexagonal benzene/phenyl rings of the MTs share three delocalized pi orbital electrons among six carbon atoms, forming "pi resonance clouds" conducive to quantum effects. Raman spectra of a microtubule and its constituent protein tubulin have shown so-called Fano resonances, which can be attributed to aromatic amino acids and disulfide bonds and are indicative of quantum coupling between discrete phonon vibrational states and continuous excitonic many-body spectra [66].

This typical electromagnetic field may organize and control the motion and transport of molecules and their components, chemical reactions, information processes, communication inside and between cells, and many other activities. A classical dipole theory has already been used of generation of the electromagnetic field to analyse the space-time coherence. The structure of microtubules with the helical and axial periodicity enables the interaction of this field in time shifted by one or more periods of oscillation and generation of coherent signals and inner cavity excitation should provide equal energy distribution in a microtubule. The supplied energy coherently excites oscillators with a high electromagnetic quality, microtubule inner cavity, and electrons at molecular orbitals in "semiconduction" and "conduction" bands. It has been proposed to be coherent

(the same frequencies, form, and phase) within the specific region: in the cell, in the tissue, and in the whole biological system and has a strongly nonlinear spectral energy transfer as predicted by Fröhlich [19] [67] [68].

In 1996, Penrose and Hameroff proposed microtubules "orchestrated" quantum superpositions, encoding inputs, and memory as entangled qubits of collective quantum dipole oscillations ("Orch"). These then compute and terminate by "orchestrated OR" ("Orch OR"), producing consciousness, and regulates the neurons. The quantum process information is considered as superpositions of multiple possibilities (quantum bits or qubits) which are collective dipole oscillations orchestrated by microtubules. These orchestrated oscillations entangle, compute, and terminate ("collapse of the wavefunction") by Penrose and Hameroff objective reduction theory. The quantum electron states resonate in microtubules at typical frequencies in the bands of: terahertz, gigahertz, megahertz and kilohertz frequencies [39]. The tubulin protein dimers of the microtubules have hydrophobic pockets that may contain delocalized π electrons and it has been claimed that this is close enough for the tubulin π electrons to become quantum entangled and the tubulin-subunit electrons would form a Bose-Einstein condensate [8]. A Fröhlich condensate has been proposed and hypothetical coherent oscillations of dipolar molecules. It is further assumed that the electrons of the mentioned pockets could represent quantum states and become quantum superposed [69], whereas these electrons represent coherent quantum superpositions, so called entangled qubits [70]. According to Orch OR hypothesis: tubulin qubits in quantum superposition interact or compute with other super-positioned tubulins in microtubule lattices by nonlocal quantum entanglement, eventually reducing to classical tubulin states. At the centre of these approaches are microtubules as the substrate on which conscious processes in terms of quantum coherence and entanglement can be built, whereas Geesink showed that also our brain frequency patterns are scale invariant [8] [31] [39].

4.2. Organizing Electromagnetic Oscillations of Microtubules

Many organizing electromagnetic typical oscillations of microtubules have already been measured. Different investigations and measurements of ordering and regulating modes for microtubules will be analysed, further discussed, and summarized:

1) Mavromatos (2011) [71]: "A role of quantum mechanics and field theory on dissipation-free energy transfer in (brain) Microtubules (MTs) have been analysed. The basic assumption was to view the cell MT as quantum electrodynamical cavities, providing sufficient isolation *in vivo* to enable the formation of electric-dipole quantum coherent solitonic states across the tubulin dimer walls. Electromagnetic interactions of the dipole moments of the tubulin dimers with the dipole quanta in the ordered water interiors of the MT play a role and are in quantum coherent cavity modes. Quantum entanglement between tubulin dimers was argued to be possible, provided there exists sufficient isolation from

other environmental cell effects. Even if the environmental decoherence implies short time scales of order of a few hundreds of fs, this is a sufficient time for some kind of quantum computation to take place in (brain) MT, so that within these time scales the cell 'quantum calculates' the optimal 'path' along which energy and signal (information) are transported most efficiently along the MT. Alignment of MT has been measured in the direction of the externally applied alternating electric field 210,000 V/m and 2 MHz frequency" [71]. The measured frequency matches with the proposed algorithm of coherent frequencies.

2) Group of Bandyopadhyay: "A self-operating time crystal model has been described: twelve classes of rhythms are proposed or reported in the brain, including microtubules, which are so-called clocks that build a time crystal. Our brain can be described by a clock architecture, a poly-time crystal, that is linked with an inside singularity or singularities in space and represents a unit lattice. Self-similarities of resonance bands have been found, that are called triplets. Typical ratios of a fractal frequency network frequency have been reported: a self-similar triplet of triplet resonance frequency pattern for the four-4 nm-wide tubulin protein, for the 25-nm-wide microtubule nanowire and 1-mu-wide axon initial segment of a neuron. In the resonance chain model, 12 brain components were considered to cover a space of 1012 orders. The triplet assembly of resonance peaks is the most dominating groups of vibrations, next to a doublet of "pentates", triplet of "pentates" in this spectrum. Dimension of dynamics for the nested time crystals have a maximum dimension of 12D and the network of clocks is mapped for all the organs, a 12 system of clocks is proposed and the twelve different dimensions in those manifolds could operate independently by combining for example $2 \times 2 \times 3$, $2 \times 3 \times 2$, and $3 \times 2 \times 2$ scalars. Three systems have been proposed in a 3D band architecture, which is self-similar: tubulins located inside the microtubule, microtubules located inside a neuron; this would mean that this system could exchange geometric information conformally, *i.e.* without losing the angular features of the geometric shape" [72] [73] [74]. Resonance peaks of microtubules have been measured that show an increase in conductivity making use of a circuit that sends an ac signal to the microtubule, while measuring the dc resistance loss. Dominant peaks were isolated as the most probable resonance peaks of the micro tubulins at for example 12, 15, 20.0, 22, 30, 101, 113, and 204 MHz, which can be related to regulation, ordering and growth of microtubules. The resonant vibrations established that the condensation of energy levels and periodic oscillation of unique energy fringes on the microtubule surface also emerging as the atomic water core resonantly integrates the MT's around it [67]. Interestingly these measured peaks precisely fit with the typical frequency positions and patterns described by the proposed scale invariant quantum equation of coherence, see **Figure 14**.

It has been concluded that the measurements of typical distinct frequency points make it possible to substantiate the proposed model of Fröhlich [68]. Remarkedly, all the measured peaks at MHz frequencies also fit with the typical

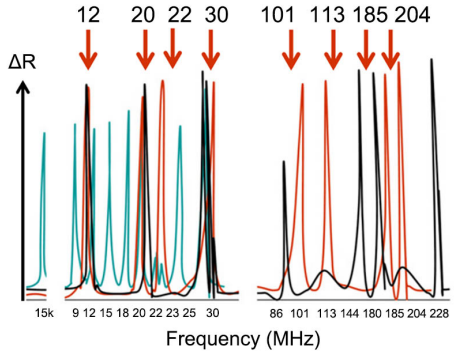

Figure 14. Typical microtubules frequencies: Resistance-loss for resonance measurements (reference: Sahu *et al*., 2013).

frequency positions and patterns calculated by the proposed scale invariant quantum equation of coherence. Also the measured peaks at GHz frequencies fit with the typical frequency calculated positions and patterns of this quantum equation of coherence, all located in a toroidal geometric order, and see **Appendix 1**.

3) Rafati *et al*. (2020) [75]: "Differentiated neuronal cells exposed to RF waves have been tuned by resonance to select frequency peaks for tubulins at 91 MHz and 281 MHz and for MTs (3.0 GHz) for 1 hr at a power density of 0.24 mW/cm^2. Fluorescence imaging has been used of endogenous MTs and current-clamp electrophysiology to investigate changes following RF exposures compared to sham. The results from the imaging data show a clear difference in the localization of fluorescent MTs between the sham and the RF exposed neuronal cells. The sham cells exhibited more fluorescence in the neurite projections, whereas the RF exposed cells showed a more diffuse pattern, with a stronger fluorescence in the cell body" [75]. The applied frequencies precisely fit with the patterns calculated by the quantum equation of coherence and see **Appendix 1**.

4) Koch *et al*. (2017) [76]: "Frequency-dependent transport of mechanical stimuli by single microtubules and small networks has been studied using optically trapped beads as anchor points. Interconnected microtubules to linear and triangular geometries have been performed applying micro-rheology by defined oscillations of the beads relative to each other. A substantial stiffening of single filaments has been found above a characteristic transition frequency in the range of 1 - 30 Hz depending on the filament's molecular composition. Below this frequency, filament elasticity only depends on its contour and persistence length. Interestingly, this elastic behaviour is transferable to small networks, where it has been found that linear two filament connections act as transistor-like, angle dependent momentum filters, whereas triangular networks act as stabilizing elements. The observations implicate that cells can tune mechanical signals by temporal and spatial filtering stronger and more flexibly than expected" [76]. The applied and measured frequencies precisely fit with the calculated patterns of the proposed quantum equation of coherence and see **Appendix 1**.

5) Pizzi *et al.* (2010) [77]: "Microtubules are claimed to be involved as sub-cellular information or quantum information communication systems, whereas MTs are the closest biological equivalent to metamaterials. Biophysical properties of MTs have been evaluated through two specific physical measures of resonance and birefringence, on the assumption that when tubulin and MTs show different biophysical behaviours, this should be due to the special structural properties of MT's. The MTs behave as oscillators and can make them reactive receivers able to amplify radio wave signals. The experimental approach was able to verify the existence of mechanical resonance in MTs at an eigenfrequency of 1510 MHz and the analysis of the results of birefringence experiment highlights that the MTs react to electromagnetic fields in a different way than a tubulin" [77]. The measured frequencies fit with the calculated pattern of the proposed quantum equation of coherence and see **Appendix 1**.

6) Li *et al.* [78]: "A molecular structural mechanics model for the microtubule structure has been employed to simulate the vibration of MTs subject to an alternating EMF generated by a dipole antenna. The vibration spectra are recorded for MTs for various possible modes. The correlation between frequency shift and the possible softening/hardening of MTs has been quantified demonstrating the potential application of vibrating MTs as biosensors. In addition, a parametric study has been conducted to evaluate the damping effect of surrounding cytosol, which could be reduced by the nanoscale MT-cytosol interface. The parametric study has been conducted for the transverse vibration of MTs across a range of damping effects and frequencies up to 50 MHz" [78] and see **Figure 15**. The observation shows that the excitations of the MT vibration with relatively large, odd half wavenumber and particularly even half wavenumbers are sensitive to the selected frequency of the EMF, and accordingly, showed narrow or sharp peaks in the amplitude-frequency spectra. The Radial Breathing Mode (RBM) with a circular cross section and the axial half wavenumber m = 1 was observed at around 53.019 MHz, whereas the circumferential modes with a non-circular cross section were found at around 585.639 MHz. The frequency 159.291 MHz of the RBM with m = 3 is three times as much as the 53.019 MHz associated with m = 1 [78]. The measured frequencies fit with the pattern of the proposed quantum equation of coherence and see **Appendix 1**.

7) Staelens *et al.* [79]: "Experimental investigations involving Photo- Biomodulation (PBM) of living cells, tubulin, and microtubules in buffer solutions exposed to Near-Infrared (NIR) light emitted from an 810 nm LED with a power density of 25 mW/cm^2 pulsed at a frequency of 10 Hz. In 45.5 μM tubulin samples it has been demonstrated that a remarkable increase in the polymerization rates and total polymer mass achieved after exposure to the PBM" [79]. The applied NIR frequency fits within the calculated bands of the proposed equation of coherence.

8) Havelka and Cifra [80]: "A strategy has been proposed for controlling tubulin self-assembly by nanosecond Electropulses (nsEPs) and it is suggested that changes in C-terminal modification states alter tubulin polymerization-competent

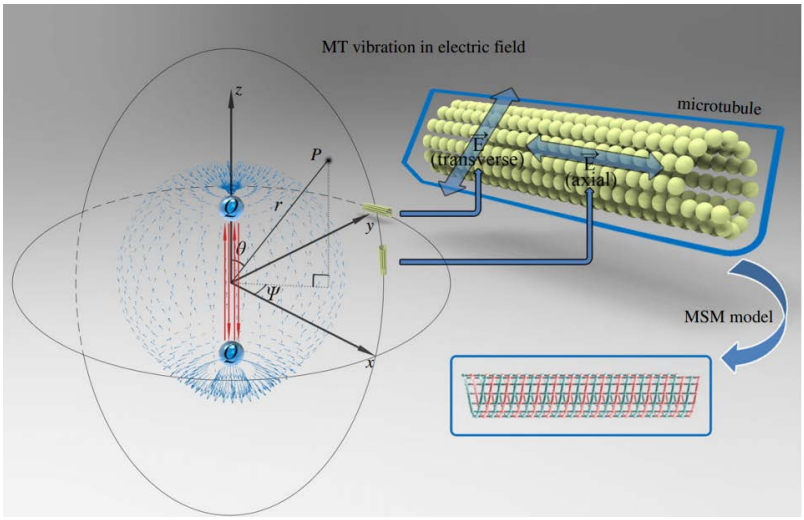

Figure 15. EF generated by a Hertzian dipole in a spherical polar coordinate system and its vector directions at the locations where the MT was placed (reference: Li *et al.*, 2019).

conformations. Although the assembled tubulin preserves their integral structure, they might exhibit a broad range of properties important for their functions. A chip platform has been developed that enables the delivery of pulsed electric field to MT systems while enabling live imaging of MTs with a TIRF microscope" [81] [82].

9) Small-signal alternating current conductance of electrolytic solutions containing MTs, and tubulin dimers have been measured using a microelectrode system. It has been found that MTs in a 20-fold diluted electrolyte increase solution conductance by 23% at 100 kHz, and this effect is directly proportional to the concentration of MTs in solution [83] [84].

10) Dotta *et al.* [85]: "Photon counts were measured every 15 ms for 75 s from microtubule-enriched preparations and nuclei from mouse melanoma cells during baseline and after 2 min exposures to 1 μT magnetic fields. The magnetic fields were generated from a circular array of solenoids and presented with accelerating or decelerating rotation velocities. The range of photon radiant flux density was in the order of 10 - 12 $W \cdot m^{-2}$. Microtubules preparations that had been exposed for 2 min to a magnetic field configuration corresponding to the electric field pattern and induced long-term potentiation in neural tissue show typical frequencies: 7 - 8 Hz, 9.5 Hz, 14 - 15 Hz, and 22 Hz. The major peak (9.4 Hz) bandwidth was approximately 0.1 Hz. The results suggest that the photon emissions from microtubule preparations have the capacity to respond to specifically patterned or geometric shapes of magnetic fields by altering spectral configurations rather than the absolute numbers of photons" [85]. The measured frequencies fit with the calculated pattern of the proposed quantum equation of coherence and see **Appendix 1**.

11) Kalra and Tuszynski *et al.* [86]: "The crystalline order in a microtubule, with lattice constants short enough to allow energy transfer between amino acid

chromophores, is similar to synthetic structures designed for light harvesting. After photoexcitation, these amino acid chromophores can transfer excitation energy along the microtubule like a natural or artificial light-harvesting system. Tryptophan autofluorescence lifetimes have been used to probe inter-tryptophan energy hopping in tubulin and microtubules. By studying how quencher concentration alters tryptophan autofluorescence lifetimes, it has been demonstrated that electronic energy can diffuse over 6.6 nm in microtubules. It has been discovered that while diffusion lengths are influenced by tubulin polymerization state, they are not significantly altered by the average number of protofilaments. The studies indicate that microtubules are, unexpectedly, effective light harvesters. The experiments reveal that energy can migrate by diffusive energy transfer over unexpectedly large distances (6.6 nm). It has been found that conventional Förster theory predicts a diffusion length of only ~2.3 nm, which is insufficient to explain these observations. Introducing the anesthetics etomidate and isoflurane decreases the observed energy diffusion length. A long pass dielectric filter with a transition wavelength of 325 nm was placed after the solution and before the detector to reduce scatter signal and the fluorescence emission was detected at 335 nm. The observations suggest that photoexcitation diffusion takes place in a manner that is dependent on the tubulin polymorph type (tubulin dimers versus oligomers versus microtubules). The observation of diffusion lengths in GMPCPP microtubules also supports the notion that a repeating arrangement of tubulin dimers is sufficient to allow long-range photoexcitation energy transfer" [86]. Interestingly the measured fluorescence emission of the microtubules detected at 335 nm precisely fits with the calculated coherent light frequency by the proposed quantum equation of coherence and see **Appendix 1**. The inner hollow volume of MT can be assumed to be "filled" with (thermally) isolated water that, undergoes a spontaneous quantum phase transition towards a coherent state in which an electromagnetic field oscillates in tune with the water matter field between two energy levels corresponding to an electronic transitions of water molecules. For the water enclosed within a cavity, as happens in MTs, it has been shown that cavity wall is able to decrease the impact of thermal fluctuations so making the interfacial water substantially thermally isolated and then much more coherent than bulk water [71] [87] [88].

Conclusions: The registered measured frequencies related to organizing resonances and typical frequencies obey to the frequency pattern described by the proposed equation of coherence, which describes quantum entangled coherent states. The mentioned measured MT-eigenfrequencies all fit with the proposed scale invariant scale within a mean average band of 1.11%. All measured MT frequencies also comply with the calculated semi-harmonic frequency patterns and values found in purified water [89] and see **Table A1** in **Appendix 6**.

4.3. Disorganising Electromagnetic Oscillations of Microtubules

Also, the disturbance of order of microtubules can be measured, and calculated

by the proposed quantum equation of decoherence. Different investigations and measurements of de-ordering and deregulating modes for microtubules will be analysed, further discussed, and summarized:

8) Hough *et al.* [15]: "Typical THz radiation at a non-ionizing level shows coupling to vibrational and rotational modes implying that external excitation with pulses of THz energy can non-thermally dysregulate structural dynamics of biomolecular structures (e.g. proteins, nucleic acids, or membrane structures) such that the associated function is compromised. At the tissue level, the effects on 3D human skin models have been investigated by measuring global differential gene expression for varying THz intensities. These data are used to determine biological processes and molecular signalling pathways that are able to be dysregulated by THz exposures, particularly focusing on dysregulation of cancer-related processes. At the molecular scale, disassembly of polymerized microtubules (rhodamine-labelled fluorescent tubulin) at a non-thermal level has been observed to occur within minutes of an applied train of THz pulses depending on the intensity and frequency content of the applied pulse. At the tissue-level, a THz exposure can induce a large differential gene expression response. THz waves with high peak electric fields at 0.5 and 1.5 THz are sufficient to induce significant non-thermal biological effects at multiple scales of biological organization. Fröhlich's model of nonlinear energy transfer in biological systems has been proposed, that explains a coherent behaviour observed in complex macromolecules like proteins" [15] [16]. The applied typical THz frequencies show a de-ordering effect and precisely fit in the pattern of the proposed quantum equation of decoherence and see **Appendix 2**.

9) Hintzsche *et al.* [90]: "Disturbance has been observed to the spindle apparatus (a mitotic structure comprised of microtubules) in hybrid animal cells. Monolayer cultures in petri dishes were exposed for 0.5 h to 0.106 THz radiation with power densities ranging from 0.043 mW/cm^2 to 4.3 mW/cm^2 or were kept under sham conditions (negative control) for the same period. Based on a total of 6365 analysed mitotic cells, the results of the replicate experiments show that 0.106 THz radiation is a spindle-acting agent as predominately indicated by the appearance of spindle disturbances at the anaphase and telophase (especially lagging and non-disjunction of single chromosomes) of cell divisions" [90]. The applied typical THz frequencies show a disorganizing effect and precisely fits in the pattern of the proposed quantum equation of decoherence and see **Appendix 2**.

10) Tuszynski and Costa [91]: It is considered that microtubules are also most likely the principal cellular bio-antenna for therapeutic electromagnetic waves due to their exceptionally high electric charge and dipole moment values directly coupling with these waves. It has been argued that the effect of exposure on microtubule ion flows may impair cell division and disrupt subcellular trafficking of mitochondria. Modulations on a 27.12 MHz carrier wave shows resonant coupling and appears to disrupt cell division and subcellular trafficking of mi-

tochondria. An estimation has been made of the contribution of the electromagnetic effects to the overall energy balance of an exposed cell by calculating the power delivered to the cell, and the energy dissipated through the cell due to EMF induction of ionic flows along microtubules. The applied typical MHz frequency shows a disorganizing effect and precisely fits in the pattern of the proposed quantum equation of decoherence and see **Appendix 2**.

Conclusions: The registered measured and applied frequencies related to disorganizing resonances/frequencies obey to the frequency pattern described by the proposed equation of decoherence, that describes quantum disentangled decoherent states.

4.4. Organizing Oscillations of DNA, Stem Cells, Genes, and Proteins

The different investigations related to ordering and regulating modes of different DNA, stem cells, genes and proteins will be summarized, further analysed, and discussed:

1) Nardecchia *et al.* [12]: "Collective oscillations of a model protein have been predicted to occur for example in the THz frequency domain. Collective oscillations of an entire molecule, or of a substantial fraction of its atoms, are essential to generate giant oscillating molecular dipole moments. These oscillations are a necessary condition to activate sizable long-distance electrodynamic interactions between resonating molecules. The measured phenomenon shows that switching on collective oscillations is out-of-thermal equilibrium. A model protein Bovine Serum Albumin has been used to show this phenomenon of such collective oscillations. The BSA protein in watery solution, when driven in a stationary out-of-thermal equilibrium state by means of optical pumping, displays a typical absorption peak around 0.314 THz and is identified as a collective oscillation of the entire molecule. These interactions could play a relevant role in regulating the dynamics of the molecular machinery at work in living matter" [12]. Interestingly the measured frequency at 0.314 THz related to regulation and order of microtubules frequencies precisely fit with the proposed quantum equation of coherence and see **Appendix 3**.

2) Tang [92]: "DNA mutations have been studied by terahertz (THz) and have been carried out to in a label-free manner. Three designed liquid sample cells have been considered and have been selected as the sample carrier for THz transmission spectroscopic analyses. Discrimination based on spectral signatures of single-base mutations on single-stranded 20 nt oligonucleotides has been shown possible experimentally. The study has demonstrated that the THz spectroscopic technology can be considered as a potential diagnostic tool for investigating molecular reactions, such as DNA mutations" [92]. The measured THz-spectra fit with the proposed equation of coherence and see **Figure A1** and **Appendix 3**.

3) Titova [93]: "The exposure of artificial human skin tissue to intense, picosecond-duration THz pulses affects expression levels of numerous genes asso-

ciated with non-melanoma skin cancers, psoriasis, and atopic dermatitis. Genes affected by intense THz pulses include nearly half of the Epidermal Differentiation Complex (EDC) members. EDC genes, which are mapped to the chromosomal human region 1q21, encode for proteins that partake in epidermal differentiation and are often overexpressed in conditions such as psoriasis and skin cancer. Human epidermal keratinocytes and dermal fibroblasts as part of artificial multilayer human skin tissue were irradiated with pulsed broad-band THz radiation (frequency 0.1 - 2.5 THz, power density 5.7 and 57 mW/cm^2) for 10 min generated by optical rectification of tilted-pulse-front 800 nm pulses from an amplified Ti: sapphire laser source in a $LiNbO_3$ crystal. The results of the study showed that terahertz radiation causes a selective reduction of the expression of the genes associated with the development of such skin diseases as psoriasis, atopic dermatitis, and other inflammatory diseases, as well as of the genes of the proteins that participate in apoptosis [94]. In nearly all the genes differentially expressed by exposure to the THz pulses, the induced changes in transcription levels are opposite to disease-related changes. The ability of THz pulses to cause concerted favourable changes in the expression of multiple genes implicated in inflammatory skin diseases and skin cancers suggests potential therapeutic applications of intense THz pulses in the broadband 0.2 - 2.5 THz" [93] [94] [95]. The applied THz frequencies: 0.55, 1.25, 1.84, 1.95, 2.30 THz and 400 nm by Titova fit with the proposed quantum equation of coherence, see **Appendix 3**.

4) Bogomazova [96]: "Human Embryonic Stem Cells (hESCs) are sensitive to environmental stimuli, and therefore a cell model has been utilised to investigate the non-thermal effects of THz irradiation. DNA damage and transcriptome responses have been studied in hESCs exposed to narrow-band THz radiation (2.3 THz) under strict temperature control. The transcription of approximately 1% of genes was subtly increased following THz irradiation. Functional annotation enrichment analysis of differentially expressed genes revealed 15 functional classes, which were mostly related to mitochondria. Terahertz irradiation did not induce the formation of γH2AX foci or structural chromosomal aberrations in hESCs. Not any effect was observed on the mitotic index or morphology of the hESCs following THz exposure. Within the ellipse, the average radiation power was 1.4 W/cm^2 and the peak radiation intensity was 4 kW/cm^2 and the average radiation power was 0.14 W/cm^2. The temperature on the OptiCell surface was kept in the range of 36.5 - 37.5 C and the warming of the irradiated samples above the room temperature of 24 C was due to the thermal effect of the THz radiation" [96]. The measured frequency of stem cells, related to regulation and ordering at 2.3 THz fits with the proposed quantum equation of coherence and see **Appendix 3**.

5) Zhao [97]: "The effects of at 3.1 THz radiation on protein expression have been explored in Escherichia coli (*E. coli*) using red fluorescent protein as a reporter molecule. After 8 hours of continuous THz irradiation of bacteria on LB (Luria-Bertani) solid plates at an average power of 33 mW/cm^2 and 10 Hz pulse

repetition frequency, it was found that the plasmid copy number, protein expression and fluorescence intensity of bacteria from the irradiated area were 3.8, 2.7, and 3.3 times higher than in bacteria from the un-irradiated area, respectively. These findings suggest that plasmid replication changed significantly in bacteria exposed to 3.1 THz radiation, resulting in increased protein expression as evidenced by increased fluorescence intensity of the RFP reporter" [97]. The applied frequencies of 3.1 THz show an ordering effect and precisely fit with the proposed quantum equation of coherence and see **Appendix 3**.

6) Lechelon and Pettini *et al.* [98] [99]: "Both classical and quantum electrodynamics predict the existence of dipole-dipole long-range electrodynamic intermolecular forces and can be observed. Experiments have been used, based on different physical effects detected by fluorescence correlation spectroscopy and terahertz spectroscopy, respectively. The activation of resonant electrodynamic intermolecular forces has been demonstrated experimentally and observed for biomacromolecules a long-range action (up to 1000 Å). Two collective oscillation frequencies for R-PE (light-harvesting protein derived from red algae) have been measured: one at 0.0714 THz and another at 0.096 THz. Similarly, the geometric shape that best fits the hexamer form of the R-PE is a torus" [99]. Both measured frequencies show an ordering effect, which fits with the proposed quantum equation of coherence, see **Figure 16**, and see **Appendix 3**.

7) Hernández-Bule *et al.* [100]: "The effects have been investigated of the exposure to a 448 kHz current typically used in so called CRET therapy, on the early chondrogenic differentiation of human, Adipose-Derived Stem Cells (ADSCs). The data set provides support to the hypothesis that the electromagnetic component of the treatment applied in CRET therapies could stimulate cartilage repair by promoting chondrogenic differentiation. The data, coupled with previously reported results that *in vitro* treatment with the same type of subthermal

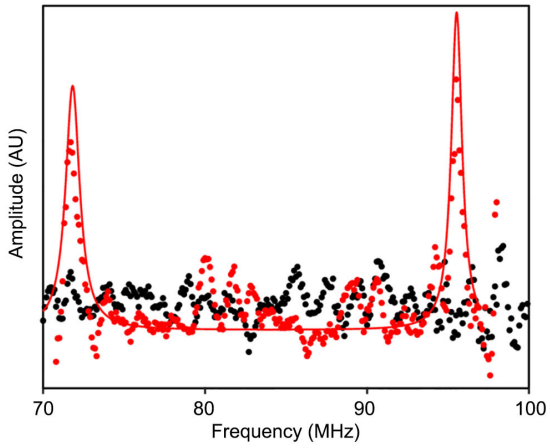

Figure 16. R-PE coherent vibrational states. Comparison of the R-PE in saline solution (red) and saline solution without R-PE (black). Two collective extension modes of R-PE appear at 71.4 and 96 GHz. Experimental data are indicated by full circles, and Lorentz fit is indicated by a solid line. AU, arbitrary units (reference: Lechelon, 2021).

electromagnetic signal promotes proliferation of undifferentiated ADSC, identify molecular phenomena underlying the potential repairing and regenerative effects of such radiofrequency currents" [100]. The applied frequencies of 448 KHz show an ordering effect and precisely fit with the proposed quantum equation of coherence [101] and see **Appendix 3**.

8) Safavi *et al.* [102]: "A meta-analysis of the influences of low-frequency Electromagnetic Fields (EMFs) on Mesenchymal Stem Cells (MSCs) can be a tool in cell therapy and tissue engineering when a regulation of stem cells is required. EMFs and PEMFs are potential modulators of MSCs differentiation and harnessing their effects may allow for improved pre-culture methods of MSCs in implantable constructs. Forty studies have been examined the effect of EMFs on MSCs osteogenic, chondrogenic, and neurogenic differentiation, and it has been shown that it may be able to improve preimplantation culture methods for seeding MSCs in biomaterials fabrication. For example, studies have shown that EMFs have positive effects on stem cell differentiation, accelerating its process regardless of the parameters and type of stem cells [103] and found that exposing human adipose-derived mesenchymal stem cells (hASCs) to a low-frequency pulsed electromagnetic fields (PEMFs) (15 Hz, 1 mT) improved their osteogenic potential. In a coculture of human osteoblasts with hASCs and exposure to extremely 16 Hz frequency promotion of osteogenic differentiation has been detected [104]. The gene expression of hASCs subjected to a low-frequency PEMFs (16 Hz) results in bone formation. Experiments to determine whether PEMFs (60 Hz) and sound waves (1 kHz) have a synergistic effect on the neurogenic differentiation of hBM-MSCs" [105] Remark: the applied frequencies are positioned at the coherent states according to the proposed quantum equation of coherence and see **Appendix 3**.

According to Pettini [106]: "The discovery of these new forces acting between biomolecules could have considerable impact on our understanding of the dynamics and functioning of the molecular machines at work in living organisms. In fact, it has been found that the model proteins used can mutually attract at a distance as large as 1000 Angstroms, which is by far larger than all the other intermolecular interactions usually considered in action in living matter. In addition to thermal fluctuations that drive molecular motions randomly, these resonant (and thus selective) electrodynamic forces may contribute to molecular encounters in the crowded cellular space".

Conclusions: The registered frequencies related to organizing resonances/frequencies obey to the frequency pattern described by the proposed equation of coherence, which describes quantum entangled coherent states. The mentioned measured DNA, stem cells, genes, and proteins organizing frequencies all fit with the proposed scale invariant scale.

4.5. Disorganizing Oscillations of DNA, Stem Cells, Genes, and Proteins

Different investigations related to de-ordering and de-regulating modes for

biomolecules will be analysed, discussed, and summarized:

6) Lundholm [9] and Ahlberg Gagnér *et al.* [10]: A model has been presented a model, which supports the model of Fröhlich condensation in the arrangement of proteins, by detecting Bose-Einstein condensate-like structures in biological matter at room temperature. The group used a combined terahertz measuring technique with a highly sensitive X-ray crystallographic method to visualize low frequency vibrational modes in the protein structure of lysozyme. The vibrations were sustained for micro- to milli-seconds, which is 3 - 6 orders of magnitude longer than expected if the structural changes would be due to a redistribution of vibrations upon terahertz absorption according to a Boltzmann's distribution. The influence of this non-thermal signal can change locally the electron density in a long alfa-helix motif, which is consistent with an observed subtle longitudinal compression of the helix. It has been found that 0.4 THz electromagnetic radiation induces non-thermal changes in electron density, combined with a local increase of electron density in a long a-helix motif consistent with a subtle longitudinal compression of the helix. These observed electron density changes occur at a low absorption rate indicating that thermalization of terahertz photons happens on a micro- to milli-second time scale, which is much slower than the expected nanosecond time scale due to damping of delocalized low frequency vibrations [9]. The anisotropy of atomic displacements increased upon terahertz irradiation (0.5 THz), whereas atomic displacement similarities developed between chemically related atoms and between atoms of the catalytic machinery. This pattern likely arises from delocalized polar vibrational modes rather than delocalized elastic deformations or rigid-body displacements. These experimental and analytical tools provide a detailed description of protein dynamics to complement the structural information from static diffraction experiments" [10]. The described experiments of protein fit with the proposed quantum equation of decoherence and see **Appendix 4**.

7) Alexandrov [107] [108]: "Low power radiation has been applied on mouse mesenchymal stem cells from both a pulsed broad-band (centred at 10 THz) source and from a CW laser (2.52 THz) source. Temperature increases were minimal, and the differential expression of the investigated heat shock proteins (HSP105, HSP90, and CPR) was unaffected, while the expression of certain other genes (Adiponectin, GLUT4, and PPARG) showed clear effects of the THz irradiation after prolonged, broad-band exposure. The level of expression of these genes in mouse stem cells remains nearly unchanged after 9 hours broad-band THz irradiation, while various other regulated genes in the same samples indicates that there is a non-thermal THz-associated mechanism that can change gene expression. The radiations were performed at biologically-low temperatures (26˚C - 27˚C), and at low THz power average densities (~1 - 3 mW/cm^2), to minimize thermal effects on the gene activity [107]. The terahertz (THz) irradiation of mouse Mesenchymal Stem Cells (mMSCs) with a Single Frequency (SF) 2.52 THz laser or pulsed broadband, centered at 10 THz source, also shows specific heterogenic changes in gene expression. The microarray survey and

RT-PCR experiments demonstrate that prolonged broadband THz irradiation drives mMSCs toward differentiation, while 2-hour irradiation (regardless of THz sources) affects genes transcriptionally active in pluripotent stem cells. The strictly controlled experimental environment indicates minimal temperature changes and the absence of any discernible response to heat shock and cellular stress genes imply a non-thermal response. It has been proposed that THz radiation at 2.52 and 10.0 THz has potential for non-contact control of cellular gene expression" [107] [108]. Interestingly both experiments of measured frequencies of the stem cells related to regulation and ordering frequencies precisely fit with the proposed quantum equation of decoherence and see **Appendix 4**.

8) Bock [109]: "Extended exposure to broad-spectrum terahertz radiation at 10.0 THz results in specific changes in cellular functions that are closely related to DNA-directed gene transcription. A gene chip survey of gene expression shows that certain genes are activated, while other are repressed. The response was not only gene specific but also irradiation conditions dependent. The findings suggest that the applied terahertz irradiation accelerates cell differentiation toward adipose phenotype by activating the transcription factor Peroxisome Proliferator-Activated Receptor Gamma (PPARG). Molecular dynamics computer simulations indicate that the local breathing dynamics of the PPARG promoter DNA coincides with the gene specific response to the THz radiation. It has been proposed that THz radiation is a potential tool for cellular reprogramming" [109]. The described experiments of gene transcriptions fit in the proposed quantum equation of decoherence and see **Appendix 4**.

9) Echchgadda [110] [111] [112]: "An increase of the expression of the genes of the thermal-shock protein, transcription regulators, cellular growth factors, and anti-inflammatory cytokines has been found 4h after a THz irradiation [113]. Although increased expression was also observed in the 'temperature control,' it was higher for almost all the genes than in the experimental group. Afterwards, in a similar experimental setup with irradiation for 40 min, changes of 531 mRNA and 66 μRNA were detected in the experimental group, versus 672 mRNA and 53 μRNA in the temperature-control group. Analysis showed that the 18 different signaling pathways in which genes participated that varied under the action of THz radiation were completely different from the 13 pathways whose genes change activity under ordinary heating [110] [111]. In a next study from this group, human keratinocytes (skin cells) were exposed for 20 min to a CW source with different frequencies: 1.4, 2.52, and 3.11 THz. keeping the power density at 44.2 mW/cm^2 for each frequency, whereas the low power density was not enough to induce a thermal response. The results showed that each frequency triggered specific metabolic or signalling pathways that were not triggered by the other frequencies [111]. The authors concluded that THz radiation can affect the expression of genes and that this influence is not associated with the temperature increase of the cells during irradiation" [112] [113] [114]. The described experiments of gene transcriptions fit in the proposed quantum equation of decoherence and see **Appendix 4**.

10) Wilmink [115]: "Cultures of human skin fibroblasts were irradiated with continuous THz radiation (2.52 THz at 84.8 mW/cm^2) for 5 - 80 min, comparing them with cells heated to 40˚C and with cells subjected to the action of a genotoxic agent—UV irradiation (λ 254 nm, P 38 W) for 3 min [114] [116]. An analysis of the mRNA 4 h after the irradiation showed that the increased expression of the genes of thermal-shock proteins had different dynamics in the test group from that for the temperature control. At the same time, no changes were observed during irradiation in the expression of the analysed genes that serve as markers of the DNA damage caused by the action of UV radiation. The authors showed that the stress response genes started to be activated when the THz-radiation power was increased (227 mW/cm^2)" [115]. The described experiments of exposed fibroblasts fit in the proposed quantum equation of decoherence and see **Appendix 4**.

Conclusions: The registered frequencies related to disorganizing resonances and frequencies of DNA, stem cells, genes, and proteins obey to the frequency pattern described by the proposed equation of decoherence, that describes quantum disentangled decoherent states.

5. Coherent Domains and Fractal Properties

According to the model of Caligiuri, brain microtubule including water trapped inside the tubules can undergo a spontaneous quantum phase transition toward a macroscopic coherent quantum state in which tubules and water molecules oscillate in phase with an EM-field, condensed from quantum vacuum, corresponding to suitable electronic transitions. This may imply the arising of macroscopic quantum "coherent domains", in which the oscillating EM-field is trapped at an evanescent-wave-like behaviour. Special dynamics of water quantum coherent domains and microtubule's walls can show some features like those characterizing artificial metamaterials allowing a superfast interaction between brain microtubules mediated by a virtual photon tunneling [88]. As the water molecule is an electrical dipole, the water in the body and in the cells possesses a polarization density P(x, t) different from zero. In such an ordered medium according to the Anderson-Higgs-Kibble (AHK) mechanism, the electromagnetic field acquires a finite mass M = M(P) while propagating, depending on the polarization [117] [118]. With P(x, t) = 0 the electromagnetic field propagates in spherical Maxwell waves. With a non-zero polarization the electromagnetic field propagates in a filamentary way piercing in a self-focusing way through the ordered medium [119] [120] [121]. The diameter of the channel depends on the mass M as d = $\hbar$/cM. The electromagnetic field E is confined within these channels, whereas its intensity is zero outside the channels. At the boundaries of these channels a transverse field gradient acts on the atoms and molecules in their environment as an attractive or repulsive force F, depending on the gradient of the field E and the matching of its frequency ν with the resonance frequencies ν_{0k} of the respective molecules and Γk the damping factor of

the molecular oscillations with the frequency ν_{0k} according to Del Giudice [122].

In this way, coherent resonance frequencies of the propagating electromagnetic field can cause a selective collection of molecules in the boundary of the channel, thus forming the dynamic cylindrical molecular structure of the microtubules, which remains stable, when the electrical field diminishes, and the molecules form stabilized positions. Such stable bounds can cause a dynamical polymerization process which underlies the dynamics of the generating electromagnetic fields. Also, the coating of the channels may explain the observed process of the dynamical formation of the cytoskeleton, which constantly changes its shape and structure. The diameter of the channels can be calculated with a mass of M = 13.60/$\sqrt{\alpha}$ eV and a fraction α of oriented water dipoles as d = 125 Å, which is exactly the observed average diameter of the microtubules [122]. The dynamical properties of the transverse and longitudinal forces along the microtubules explain observed effects as their spontaneous formation and dissolution as well as the observed treadmilling [123]. These dynamical processes, which can construct and deconstruct the cytoskeleton, depend sensitively on the resonance quality of signals which interact with it. If an external signal possess coherence through its self-similar fractal properties, its effect on the microtubules will be constructive while non-coherent signals may influence the cytoskeleton negatively. Coherent sounds may for example increase the coherence and non-coherent dissonant sounds may obstruct the coherence of living biological matter as the cytoskeleton and its microtubules [118].

In quantum physics, the property of complementarity of non-interchangeable observables such as location and momentum can be related to a wave function in the complex number space. The property of complementarity corresponds to the representation by complex numbers, since only the special calculus properties of complex numbers enable the common definition of complementary property spaces. Health can be understood as the coherence of the human being including his organism, mind, and relationship to his environment. Quantum entanglement of subsystems on all levels of the human being is responsible for the wholeness of the living entity. The sum of entanglements can be defined as a so-called Information Field and entangled frequencies can resonate with and influence human bioenergetic processes and systems with the aim of creating coherence of the bioenergetic system, both within the individual and between the individual and the surrounding fields according to Schmieke [124].

6. Discussions and Conclusions

The necessity of using quantum mechanics as a fundamental theory applicable to some key functional aspects of biological systems has been considered. This is especially relevant to three important parts of a neuron in the human brain, namely the cell membrane, Microtubules (MTs), and ion channels. To have a very high degree of coherence between biomolecules, Bose-Einstein condensation may be a viable mechanism [125] [126]. In quantum physics, the property

of complementary non-interchangeable observables such as location can be related to a wave function in the complex number space. Different studies of frequency measurements of microtubules and DNA, stem cells, and proteins have been analysed, that show measured frequency positions that can be described by a proposed quantum wave equation of coherence (regulation) or decoherence (deregulation). A literature survey was performed on intrinsic frequencies and frequencies of microtubules of different studies measured across the electromagnetic spectrum using various spectroscopic technologies.

A fit has been found for about 50 typical organizing frequencies and 5 disorganizing frequencies of measured microtubule cell frequencies and fits with the calculated discrete values of the proposed quantum equations, that describe a nested toroidal geometry, see also **Appendix 5**. The registered frequencies obey to the frequency pattern of the proposed scale-invariant quantum equations of coherence and decoherence, which respectively describes quantum entangled states or disentangled states, and can be compared with earlier detected electromagnetic frequency patterns revealed in various biological systems. The same relation of coherent (healthy) or decoherent (unhealthy) frequency patterns of different studies also has been for stem cells, proteins, and gene transcriptions, see **Appendix 6**.

The meta-analysis of microtubules shows that the same semi-harmonic frequency pattern can be found for Bose-Einstein condensates. A fit has been found for about 86 different measured microtubule frequencies, including stem cells, DNA, and different proteins, see **Appendix 5** and **Appendix 6**. Interestingly, the same fit could be found for the analysed scale-invariant discrete brain frequencies measured by EEG and MEG, which show coherent or decoherent frequency patterns, that can be substantiated by the same quantum physical model about phase-synchronisation and quantum entanglement [31] [32] [33].

The necessity of using quantum mechanics as a fundamental theory applicable to some key functional aspects of biological systems proposed by Fröhlich, Tuszynski, Katona, Pettini, Bandyopadhyay, Del Giudice, Vitiello, and many others can be substantiated. This is especially relevant to three important parts of a neuron in the human brain, namely the cell membrane, and microtubules. To have a very high degree of coherence between biomolecules, Bose-Einstein condensation plays a viable mechanism. Many independent experiments related to the energy distributions of Bose-Einstein condensates show a semi-harmonic distribution of energies (78 data in 26 publications of Geesink [22], see **Figure A2**) and fit with the proposed energy distribution of microtubules. All measured and analysed frequencies of microtubules as well as energies/frequencies of Bose-Einstein condensates can be normalized into the same distribution of 12 positions of an invariant frequency scale, that represents coherent frequencies in the bands of Hz, Khz, MHz, Thz, and PHz, see **Appendix 6** and **Appendix 7**.

There may be also a relation with energy sources to maintain biomolecules in these ordered states, whereas possible candidates are: Adenosine Triphosphate

(ATP) as a universal biological fuel, ionic currents such as those used to drive ATP synthesis, ionic assemblies, and water molecules. Interestingly a relation has been found with the eigenfrequencies of ATP: at 0.42 eV energy, released under hydrolysis of ATP molecule, as studied by Davydov [47] and Pang [127] [128]. A hypothesis is that this energy is transferred along the alfa-helical protein molecules, while the oscillation energy of the C = O moieties of the peptide groups (amide-I vibration) is at 0.21 eV or 1665 cm^{-1}, which is in resonance with the 0.42 eV of the ATP process. Interestingly, the energy released under hydrolysis of ATP molecule, the oscillation energy of the C = O of the peptide groups, and the different bending modes of interfacial water molecules fit with the calculated coherent frequencies of the proposed quantum equation of coherence, respectively: 0.415 eV, 0.2073 eV, and 1660 - 1693 cm^{-1}. It is well-known that water plays a necessary and key role, and a frequency spectra formula for biomolecules has been derived, starting with water, which is represented by a toroidal structure, such that other elements essential to life, such as oxygen, carbon, nitrogen, and hydrogen can all be fitted into the same formula, dividing it into coherent and de-coherent states according to Wong [17] [129]. A meta-analysis of about 700 measured frequencies of pure water shows that 192 subsequent first and second derivatives of spectral frequency curves of water molecules can be precisely positioned at the proposed lines of the calculated pattern of coherent eigenfrequencies with an error of 0.45% and statistical significance of $p < 0.02$ [89].

Interestingly mineral/biochip electromagnetic technology is under development to stabilize this kind of organisation of biomolecules and cells by adding or emitting coherent waves to improve healthy coherent electromagnetic resonances of living molecules and cells. Therefore, templated nanocrystal assemblies can generate typical electromagnetic fields to organize and control the motion and transport, assembly, and growth of molecules and are characterized by their frequency patterns [28] [130] [131]. Semi-conductors based on for example phyllosilicate minerals are a candidate to make signals biocompatible with signals of living cells. The silicate mineral can be incorporated into a biochip to generate and emit typical multi-quantum coherent waves at infrared frequencies, and mimic the multiple discrete frequencies of Bose-Einstein condensates, related to frequency patterns of biomolecules, or called organising electromagnetic waves [132].

The different calculations of coherent/regulating and decoherent/deregulating patterns are presented in **Appendices 1-4**: Mavromatos [71]; Sahu [67] [68]; Saxena [73]; Rafati [75]; Koch [76]; Pizzi [77]; Li [78]; Barlow [133]; Palalle [134]; Romanenko [135]; Chafai [81]; Hameroff [8]; Dotta [85]; Kalra [86]; Hough [136]; Hintzsche [90]; Cantero [63]; Tuszynski [91]; Nardecchia [12]; Tang [92]; Titova [93] [94] [95]; Bogomazova [96]; Zhao [97]; Lechelon [99]; Hernández-Bule [101]; Safavi [102]; Lundholm [9]; Ahlberg Gagnér [10]; Alexandrov [107] [108]; Bock [109]; Echchgadda [110] [111]; Wilmink [114] [115] [116]; Grundt [113];

Tachizaki [137]; Romanenko [138].

Acknowledgements

We are grateful for the discussions with Kai-Wai Wong, Prof. em. of the Dept. Physics and Astronomy, University of Kansas, USA, and Dick Meijer, Prof. em. of the University of Groningen.

Conflicts of Interest

The authors declare no conflicts of interest regarding the publication of this paper.

Conflicts of Interest

The authors declare no conflicts of interest regarding the publication of this paper.

References

[1] Fröhlich, H. (1968) *Journal of Quantum Chemistry*, **2**, 641-649. https://doi.org/10.1002/qua.560020505

[2] Davydov, A.S. (1977) *Journal of Theoretical Biology*, **66**, 379-387. https://doi.org/10.1016/0022-5193(77)90178-3

[3] Wu, T.M. and Austin, S. (1978) *Journal of Theoretical Biology*, **71**, 209-214. https://doi.org/10.1016/0022-5193(78)90267-9

[4] Del Giudice, E., Doglia, S. and Vitiello, G. (1983) *Physics Letters A*, **95**, 508-510. https://doi.org/10.1016/0375-9601(83)90509-1

[5] Reimers, J.R., McKemmish, L.K., Mc Kenzie, R.H., Mark, A.E. and Hush, N.S. (2009) *PNAS*, **106**, 4219-4224. https://doi.org/10.1073/pnas.0806273106

[6] Chukova, Y.P. (2011) *Journal of Physics*: *Conference Series*, **329**, Article ID: 012032. https://doi.org/10.1088/1742-6596/329/1/012032

[7] Vasconcellos, A.R., Vannuchi, F.S., Mascarenhas, S. and Luzzi, R. (2012) *Information*, **3**, 601-620. https://doi.org/10.3390/info3040601

[8] Hameroff, S.R., Craddock, T.J.A. and Tuszynski, J.A. (2014) *Journal of Integrative Neuroscience*, **13**, 229-252. https://doi.org/10.1142/S0219635214400093

[9] Lundholm, I.V., Rodilla, H., Wahlgren, W.Y., Duelli, A., Bourenkov, G., Vukusic, J., Friedman, R., Stake, J., Schneider, T. and Katona, J. (2015) *Structural Dynamics*, **2**, Article ID: 054702. https://doi.org/10.1063/1.4931825

[10] Ahlberg Gagnér, A., Lundholm, V.I., Garcia-Bonete, M.J., Rodilla, H., Friedman, R., Zhaunerchyk, V., Bourenkov, G., Schneider, T., Stake, J. and Katon, G. (2019) *Scientific Reports*, **9**, Article No. 19281. https://doi.org/10.1038/s41598-019-55777-5

[11] De Ninno, A. and Pregnolato, M. (2016) *Electromagnetic Biology and Medicine*, **36**, 115-122. https://doi.org/10.1080/15368378.2016.1194293

[12] Nardecchia, I., Torres, J., Lechelon, M.J., Varani, L., Donato, I., Gori, M. and Pettini, M. (2017) Out-of-Equilibrium Collective Oscillations of a Model Protein in the THz Frequency Domain. ArXiv, 1705.07975.

[13] Kadantsev, V.N. and Goltsov, A. (2019) Collective Excitations in Alpha-Helical Protein Structures Interacting with Environment. https://doi.org/10.1101/457580

[14] Scully, M.O. (2019) The Quantum Theory of the Laser and Its Application to Bose Condensates, Unruh Radiation, and Fröhlich Protein Phase Transitions. https://doi.org/10.1364/CQO.2019.Tu4B.2

[15] Hough, C.M., Purschke, D.N., Huang, C., Titova, L.V., Kovalchuk, O., Warkentin, B.J. and Hegmann, F.A. (2018) *Journal of Infrared, Millimeter, and Terahertz Waves*, **39**, 887-898. https://doi.org/10.1007/s10762-018-0512-4

[16] Hough, C.M., Purschke, D.N., Huang, C., Titova, L.V., Kovalchuk, O., Warkentin, B.J. and Hegmann, F.A. (2018) *Terahertz Science and Technology*, **11**, 28-33.

[17] Wong, K.W., Fung, P.C.W. and Chow, W.K. (2019) *Journal of Modern Physics*, **10**, 1548-1565. https://www.scirp.org/journal/jmp https://doi.org/10.4236/jmp.2019.1013103

[18] Zhedong, Z., Agarwal, G.S. and Scully, M.O. (2019) *Physical Review Letters*, **122**, Article ID: 158101.

[19] Pokorný, J., Pokorný, J. and Vrba, J. (2019) Electromagnetic Communication between Cells through Tunnelling Nanotubes. 2019 *European Microwave Conference in Central Europe* (*EuMCE*), Prague, 13-15 May 2019, 512-515.

[20] Pokorný, J., Pokorný, J. and Vrba, J. (2021) *International Journal of Molecular Sciences*, **22**, Article No. 8215. https://doi.org/10.3390/ijms22158215

[21] Geesink, J.H. and Meijer, D.K.F. (2017) *Electromagnetic Biology and Medicine*, **36**, 357-378. https://doi.org/10.1080/15368378.2017.1389752

[22] Geesink, J.H. (2020) Proposed Informational Code of Biomolecules and Its Building Blocks: Quantum Coherence versus Decoherence.

[23] Cui, Y., Liu, X.Y., Ma, X.F., Deng, Liu, Y.Y., Li, Z.Q. and Wang, Z.W. (2022) Infrared Optical Absorption of Fröhlich Polaron in Metal Halide Perovskites. ArXiv, 2201.06360. https://doi.org/10.1088/1674-1056/aca7f0

[24] Khrennikov, A. (2021) *The International Journal of Systems & Cybernetics*, **51**, 138-155. https://doi.org/10.1108/K-10-2021-0932

[25] Fröhlich, H. (1986) *Physics Letters A*, **110**, 480-481. https://doi.org/10.1016/0375-9601(85)90561-4

[26] Fröhlich, H. (1988) Biological Coherence and Response to External Stimuli. Springer, Berlin. https://doi.org/10.1007/978-3-642-73309-3

[27] Geesink, J.H. and Meijer, D.K.F. (2017) *Quantum Biosystems*, **8**, 1-16.

[28] Geesink, J.H. (2022) Informational Code for Quantum and Living Systems: Chern Numbers Normalized into Twelve n-Component Groups.

[29] Fröhlich, H. (1978) *IEEE Transactions on Microwave Theory and Techniques*, **26**, 613-618. https://doi.org/10.1109/TMTT.1978.1129446

[30] Geesink, J.H. (2021) A Predictive Quantum Model That Reveals a Causal Relation between Exposures to Non-Thermal Electromagnetic Waves and Biological Effects.

[31] Geesink, J.H. (2022) Spatio-Spectral Eigenmodes and the Toroidal Nature of Brain Waves Described by an Informational Quantum Code, Part 1.

[32] Geesink, J.H. (2022) Multiscale Dynamics of the Brain and Repetitive Electromagnetic Stimulations, Part 2.

[33] Geesink, J.H. (2022) Examples of Spatio-Spectral Brain Waves Related to Healthy and Unhealthy States Including rTMS, Part 3.

[34] Vitiello, G. (2012) *Physics Letters* A, **376**, 2527-2532. https://doi.org/10.1016/j.physleta.2012.06.035

[35] Bischof, M. and Del Giudice, E. (2013) *Molecular Biology International*, **2013**, Ar-

ticle ID: 987549. https://doi.org/10.1155/2013/987549

[36] Vitiello, G. (2012) *Journal of Physics*: *Conference Series*, **380**, Article ID: 012021. https://doi.org/10.1088/1742-6596/380/1/012021

[37] Schmieke, M. (2021) *Dev Sanskriti Interdisciplinary International Journal*, **17**, 1-12. https://doi.org/10.36018/dsiij.v17i.206

[38] Günther, G. (1976) Cybernetic Ontology Operations. Beiträge zur Grundlegung einer Operations Fähigen Dialektik, Erster Band, Felix Meiner Verlag, Hamburg.

[39] Günther, G. (1991) Metaphysik, Die Aristotelische Logik des Seins. Beiträge zur Grundlegung einer Operations Fähigen Dialektik, Band 1, Felix Meiner Verlag, Hamburg, S185-S186.

[40] Hameroff, S.R. and Orch, O.R. (2021) *Cognitive Neuroscience*, **12**, 74-76. https://doi.org/10.1080/17588928.2020.1839037

[41] Vitiello, G. (1995) *International Journal of Modern Physics B*, **9**, 973-989. https://doi.org/10.1142/S0217979295000380

[42] Freeman, W.J. and Vitiello, G. (2008) *Journal of Physics A*: *Mathematical and Theoretical*, **41**, Article ID: 304042. https://doi.org/10.1088/1751-8113/41/30/304042

[43] Hull, D. and Bacon, D.J. (2001) Introduction to Dislocations. Butterworth-Heinemann, Oxford. https://doi.org/10.1016/B978-075064681-9/50002-X

[44] Geesink, J.H. (2022) Spatio-Spectral Eigenmodes and the Toroidal Nature of Brain Waves Described by an Informational Quantum Code, Part 4.

[45] Meijer, D.K.F. and Geesink, J.H. (2018) *Journal of Cancer Therapy*, **9**, 188-230. https://doi.org/10.4236/jct.2018.93019

[46] Geesink, J.H. and Meijer, D.K.F. (2018) *Journal of Modern Physics*, **9**, 851-897. https://doi.org/10.4236/jmp.2018.95055

[47] Geesink, J.H. and Meijer, D.K.F. (2018) *Journal of Modern Physics*, **9**, 898-924. https://doi.org/10.4236/jmp.2018.95056

[48] Davydov, A.S. (1973) *Journal of Theoretical Biology*, **38**, 559-569. https://doi.org/10.1016/0022-5193(73)90256-7

[49] Fröhlich, H. (1969) Quantum Mechanical Concepts in Biology. In: Marois, M., Ed., *From Theoretical Physics to Biology*, North-Holland, Amsterdam, 13-22.

[50] Amiot, E. (2013) The Torii of Phases. In: Yust, J., Wild, J. and Burgoyne, J.A., Eds., *Mathematics and Computation in Music*, Lecture Notes in Computer Science, Vol. 7937, Springer, Berlin, 1-18.

[51] Lawo, S., Hasegan, M., Gupta, G.D. and Pelletier, L. (2012) *Nature Cell Biology*, **14**, 1148-1158. https://doi.org/10.1038/ncb2591

[52] Nygrena, J., Adelman, R.A., Myakishev-Rempel, M., Sun, G., Li, J. and Zhao, Y. (2020) *Biosystems*, **197**, Article ID: 104210. https://doi.org/10.1016/j.biosystems.2020.104210

[53] Ellis, P.W., Pearce, D.J.G., Chang, Y.W., Goldsztein, G., Giomi, L. and Fernandez-Nieves, A. (2017) *Nature Physics*, **14**, 85-90. https://doi.org/10.1038/nphys4276

[54] Zhao, Y. and Zhan, Q. (2012) *Zhao and Zhan Theoretical Biology and Medical Modelling*, **9**, Article No. 26. http://www.tbiomed.com/content/9/1/26 https://doi.org/10.1186/1742-4682-9-27

[55] Belyaev, I.Y. (2015) Biophysical Mechanisms for Nonthermal Microwave Effects. In: Markov, M.S., Ed., *Electromagnetic Fields in Biology and Medicine*, CRC Press, Boca Raton, 49-68.

[56] Blank, M. and Findl, E. (1970) Mechanistic Approaches to Interactions of Electric

and Electromagnetic Fields with Living Systems. Springer Science + Business Media, Berlin.

[57] Romanenko, S., Begley, R., Harve, A.R., Hool, L. and Wallace, V.P. (2017) *Journal of the Royal Society Interface*, **14**, Article ID: 20170585. https://doi.org/10.1098/rsif.2017.0585

[58] Adey, W.R. (1993) *Journal of Cellular Biochemistry*, **51**, 410-416. https://doi.org/10.1002/jcb.2400510405

[59] Illinger, K.H. (2016) Electromagnetic-Field Interaction with Biological Systems in the Microwave and Far-Infrared Region.

[60] Illinger, K.H. (1981) Biological Effects of Nonionizing Radiation. American Chemical Society, Washington DC, 342 p. https://doi.org/10.1021/bk-1981-0157

[61] Bornens, M. and Azimzadeh, J. (2008) *Advances in Experimental Medicine and Biology*, **607**, 119-129.

[62] Dogterom, M. and Koenderink, G.H. (2019) *Nature Reviews Molecular Cell Biology*, **20**, 38-54. https://doi.org/10.1038/s41580-018-0067-1

[63] Cantero, M.D.R., Etchegoyen, C.V., Perez, P.L., Scarinci, N. and Cantiello, H.F. (2018) *Scientific Reports*, **8**, Article No. 11899. https://doi.org/10.1038/s41598-018-30453-2

[64] Craddock, T.J.A., Tuszynski, J.A. and Hameroff, S. (2012) *PLOS Computational Biology*, **8**, e1002421. https://doi.org/10.1371/journal.pcbi.1002421

[65] Tuszynski, J.A., Friesen, D., Freedman, H., Sbitnef, V.I., Kim, H., Santelices, I., Kalra, A.P., Patel, S.D., Shankar, K. and Chua, L.O. (2020) *Scientific Reports*, **10**, Article No. 2108. https://doi.org/10.1038/s41598-020-58820-y

[66] Zhang, W., Craddock, T.J.A., Li, Y., Swartzlander, M., Alfano, R.R. and Shi, L. (2022) *Biophysical Reports*, **2**, Article ID: 100043. https://doi.org/10.1016/j.bpr.2021.100043

[67] Sahu, S., Ghosh, S., Ghosh, B., Aswani, K., Hirata, K., Fujita, D. and Bandyopadhyay, A. (2013) *Biosensors and Bioelectronics*, **47**, 141-148. https://doi.org/10.1016/j.bios.2013.02.050

[68] Sahu, S., Ghosh, S., Fujita, D. and Bandyopadhyay, A. (2014) *Scientific Reports*, **4**, Article No. 7303. https://doi.org/10.1038/srep07303

[69] McFadden, J. (2020) *Neuroscience of Consciousness*, **2020**, niaa016. https://doi.org/10.1093/nc/niaa016

[70] Brodziak, A. (2013) *Medical Science Monitor*, **19**, 1146-1158. https://doi.org/10.12659/MSM.889587

[71] Mavromatos, N.E. (2011) *Journal of Physics*: *Conference Series*, **329**, Article ID: 012026. https://doi.org/10.1088/1742-6596/329/1/012026

[72] Singh, P., Saxena, K., Singhania, A., Sahoo, P., Ghosh, S., Chhajed, R., Ray, K., Fujit, D. and Bandyopadhyay, A. (2020) *Information*, **11**, Article No. 238. https://doi.org/10.3390/info11050238

[73] Saxena, K., Singh, P., Sahoo, p., Sahu, S., Ghosh, S., Ra, K., Fujita, D. and Bandyopadhyay, A. (2020) *Fractal and Fractional*, **4**, Article No. 11. https://doi.org/10.3390/fractalfract4020011

[74] Bandyopadhyay, A. and Ray, K. (2020) Rhythmic Oscillations in Proteins to Human Cognition. Springer Nature, Berlin, 361 p. https://doi.org/10.1007/978-981-15-7253-1

[75] Rafati, Y., Cantu, J.C., Sedelnikova, A., Tolstykh, G.P., Peralta, X.G., Valdez, C. and

Echchgadda, I. (2020) *Proceedings of the SPIE*, **11238**, 112381E.

[76] Koch, M.D., Schneider, N., Nick, P. and Rohrbach, A. (2017) *Scientific Reports*, **7**, Article No. 4229. https://doi.org/10.1038/s41598-017-04415-z

[77] Pizzi, R., Strini, G., Fiorentini, S., Pappalardo, V. and Pregnolato, M. (2010) Evidences of New Biophysical Properties of Microtubules. In: Kwon, S.J., Ed., *Artificial Neural Networks*, Nova Science Publishers, Inc., Hauppauge, 1-17.

[78] Li, S., Wang, C. and Nithiarasu, P. (2019) *Journal of the Royal Society Interface*, **16**, Article ID: 20180826. https://doi.org/10.1098/rsif.2018.0826

[79] Staelens, M., Di Gregorio, E., Kalra, A.P., Le, H.T., Hosseinkhah, N., Karimpoor, M., Lim, L. and Tuszynski, J.A. (2022) *Frontiers in Medical Technology*, **4**, Article ID: 871196. https://doi.org/10.3389/fmedt.2022.871196

[80] Havelka, D. and Cifra, M. (2009) *Acta Polytechnica*, **49**, 58-63. https://doi.org/10.14311/1125

[81] Chafai, D.E., Sulimenko, V., Havelka, D., Kubínová, L., Dráber, P. and Cifra, M. (2019) *Advanced Materials*, **31**, Article ID: 1903636. https://doi.org/10.1002/adma.201903636

[82] Havelka, D., Zhernov, I., Teplan, M., Lánský, Z., Chafai, D.E. and Cifra, M. (2022) *Scientific Reports*, **12**, Article No. 2462. https://doi.org/10.1038/s41598-022-06255-y

[83] Santelices, I.B., Friesen, D.E., Bell, C., Hough, C.M., Xiao, J., Kalra, A., Kar, P., Freedman, H., Rezania, V., Lewis, J.D., Shankar, K. and Tuszynski, J.A. (2017) *Scientific Reports*, **7**, Article No. 9594. https://doi.org/10.1038/s41598-017-09323-w

[84] Kalra, A.P., Eakins, B.B., Patel, S.H., Ciniero, G., Rezania, V., Shankar, K. and Tuszynski, J.A. (2020) *ACS Nano*, **14**, 16301-1620. https://doi.org/10.1021/acsnano.0c06945

[85] Dotta, B.T., Vares, D.A.E., Buckner, C.A., Lafrenie, R.M. and Persinger, M.A. (2014) *Open Journal of Biophysics*, **4**, 112-118. https://doi.org/10.4236/ojbiphy.2014.44013

[86] Kalra, A.P., Benny, A., Travis, S.M., Zizzi, E.A., Morales-Sanchez, A., Oblinsky, D.G., Craddock, T.J.A., Hameroff, S.R., MacIver, M.B., Tuszyński, J.A., Petry, S., Penrose, R. and Scholes, G.D. (2022) Electronic Energy Migration in Microtubules. ArXiv, 2208.10628.

[87] Del Giudice, E., Stefanini, P., Tedeschi, A., *et al.* (2011) *Journal of Physics: Conference Series*, **329**, Article ID: 012001. https://doi.org/10.1088/1742-6596/329/1/012001

[88] Caligiuri, L.M. (2022) QED Coherence and Super-Coherence of Water in Brain Microtubules and Quantum Hypercomputation. In: Bandyopadhyay, A. and Ray, K., Eds., *Rhythmic Advantages in Big Data and Machine Learning*, Springer, Berlin, 225-262. https://doi.org/10.1007/978-981-16-5723-8_9

[89] Geesink, J.H., Jerman, I. and Meijer, D.K.F. (2020) *Water*, **11**, 78-108.

[90] Hintzsche, H., Jastrow, C. and Kleine-Ostmann, T. (2011) *Radiation Research*, **175**, 569-574. https://doi.org/10.1667/RR2406.1

[91] Tuszynski, J.A. and Costa, F. (2022) *Frontiers in Medical Technology*, **4**, Article ID: 869155. https://doi.org/10.3389/fmedt.2022.869155

[92] Tang, M., Huang, Q., We, D., Zha, G., Chang, T., Ko, K., Wang, M., Du, C., Fu, W. and Cui, H.L. (2015) *Journal of Biomedical Optics*, **20**, Article ID: 095009. https://doi.org/10.1117/1.JBO.20.9.095009

[93] Titova, L.V., Ayesheshim, A.K., Golubov, A., Rodriguez-Juarez, R., Kovalchuk, A., Hegmann, F.A. and Kovalchuk, O. (2013) *Scientific Reports*, **3**, Article No. 2363.

https://doi.org/10.1038/srep02363

[94] Titova, L.V., Ayesheshim, A.K., Golubov, A., Rodriguez-Juarez, R., Kovalchuk, A., Hegmann, F.A. and Kovalchuk, O. (2013) *Biomedical Optics Express*, **4**, 559-568. https://doi.org/10.1364/BOE.4.000559

[95] Titova, L.V., Ayesheshim, A.K., Golubov, A., Rodriguez-Juarez, R., Kovalchuk, A., Hegmann, F.A. and Kovalchuk, O. (2013) *Scientific Reports*, **3**, Article No. 2363. https://doi.org/10.1038/srep02363

[96] Bogomazova, A.N., Vassina, E.M., Goryachkovskaya, T.M., Popik, V.M., Sokolov, A.S., Kolchanov, N.A., Lagarkova, M.A., Kiselev, S.L. and Peltek, S.E. (2015) *Scientific Reports*, **5**, Article No. 7749. https://doi.org/10.1038/srep07749

[97] Zhao, J., Hu, E., Shang, S., Wu, D., Li, P., Zhang, P., Tan, D. and Lu, X. (2020) *Biomedical Optics Express*, **11**, 3890-3899. https://doi.org/10.1364/BOE.392838

[98] Lechelon, M. (2017) Long-Range Electrodynamic Interactions among Biomolecules. These de Doctorat, Universite d'Aix-Marseille Faculte des Sciences de Luminy Ecole doctorale de Physique et Sciences de la Matiere.

[99] Lechelon, M., Meriguet, Y., Gori, M., Ruffenach, S., Nardecchia, I., Floriani, E., Coquillat, D., Teppe, F., Mailfert, S., Marguet, D., Ferrier, P., Varani, L., Sturgis, J., Torres, J. and Pettini, M. (2022) *Science Advances*, **8**, eabl5855. https://doi.org/10.1126/sciadv.abl5855

[100] Hernández-Bule, M.L., Trillo, A.M., Martínez-García, A., Abilahoud, C. and Úbeda, A. (2017) *Journal of Stem Cell Research & Therapeutics*, **7**, Article ID: 1000407. https://doi.org/10.4172/2157-7633.1000407

[101] Hernández-Bule, M.L., Paíno, C.L., Trillo, M.A. and Úbeda, A. (2014) *Cellular Physiology and Biochemistry*, **34**, 1741-1755. https://doi.org/10.1159/000366375

[102] Safavi, A.S., Sendera, A., Haghighipour, N. and Banas-Zabczyk, A. (2022) *Tissue Engineering and Regenerative Medicine*, **19**, 1147-1160. https://doi.org/10.1007/s13770-022-00473-1

[103] Aldebs, A., Zohora, F.T., Nosoudi, N., Singh, S.P. and Ramirez-Vick, J.E. (2020) *Bioelectromagnetics*, **41**, 175-187. https://doi.org/10.1002/bem.22248

[104] Ehnert, S., Van Griensven, M., Unger, M., Scheffler, H., Falldorf, K., Fentz, A.K., *et al.* (2018) *International Journal of Molecular Sciences*, **19**, Article No. 994. https://doi.org/10.3390/ijms19040994

[105] Choi, Y.K., Lee, D.H., Seo, Y.K., Jung, H., Park, J.K. and Cho, H. (2014) *Applied Biochemistry and Biotechnology*, **174**, 1233-1245. https://doi.org/10.1007/s12010-014-1091-z

[106] Pettini, M. (2022) Lecture: Long-Distance Electrodynamic Interactions among Biomolecules. Center for Theoretical Physics and Aix-Marseille University Luminy, Marseille.

[107] Alexandrov, B.S., Rasmussen, K.Ø., Bishop, A.R., Usheva, A., Alexandrov, L.B., Chong, S., Dagon, Y., Booshehri, L.G., Mielke, C.H., Phipps, M.L., Martinez, J.S., Chen, H.T. and Rodriguez, G. (2011) *Biomedical Optics Express*, **2**, 2679-2689. https://doi.org/10.1364/BOE.2.002679

[108] Alexandrov, B.S., Phipps, M.L., Alexandrov, L.B., Booshehri, L.G., Erat, A., Zabolotny, J., Mielke, C.H., Chen, H.T., Rodriguez, G., Rasmussen, K.O., Martinez, J.S., Bishop, A.R. and Usheva, A. (2013) *Scientific Reports*, **3**, Article No. 1184. https://doi.org/10.1038/srep01184

[109] Bock, J., Fukuyo, Y., Kang, S., Phipps, M.L., Alexandrov, L.B., Rasmussen, K.O., Bishop, A.R., Rosen, E.D., Martinez, J.S., Chen, H.T., Rodriguez, G., Alexandrov, B.S.

and Usheva, A. (2010) *PLOS ONE*, **5**, e15806. https://doi.org/10.1371/journal.pone.0015806

[110] Echchgadda, Grundt, J.E., Cerna, C.Z., Roth, C.C., Ibey, B.L. and Wilmink, G.J. (2014) Terahertz Stimulate Specific Signaling Pathways in Human Cells. 39*th International Conference on Infrared*, *Millimeter*, *and Terahertz Waves*, Tucson, 14-19 September 2014, 1-2. https://doi.org/10.1109/IRMMW-THz.2014.6956140

[111] Echchgadda, Cerna, C.Z., Sloan, M.A., Elam, D.P. and Ibey, B.L. (2015) Effects of Different Terahertz Frequencies on Gene Expression in Human Keratinocytes. *Optical Interactions with Tissue and Cells XXVI*, Vol. 9321, 147-155. https://doi.org/10.1117/12.2082542

[112] Echchgadda, *et al.* (2016) *IEEE Transactions on Terahertz Science and Technology*, **6**, 54-68. https://doi.org/10.1109/TTHZ.2015.2504782

[113] Grundt, J.E., Cerna, C., Roth, C.C., Ibey, B.L., Lipscomb, D., Echchgadda, I. and Wilmink, G.J. (2011) Terahertz Radiation Triggers a Signature Gene Expression Profile in Human Cells. *International Conference on Infrared*, *Millimeter*, *and Terahertz Waves*, Houston, 2-7 October 2011, 1-2. https://doi.org/10.1109/irmmw-THz.2011.6104967

[114] Wilmink, G.J., Rivest, B.D., Roth, C.C., Ibey, B.L., Payne, J.A., Cundin, L.X., Grundt, J.E., Peralta, X., Mixon, D.G. and Roach, W.P. (2011) *Lasers in Surgery & Medicine*, **43**, 152-163. https://doi.org/10.1002/lsm.20960

[115] Wilmink, G.J., Rivest, B.D., Ibey, B.L., Roth, C.C., Bernhard, J. and Roach, W.P. (2010) *Lasers in Surgery & Medicine*, **7562**, 75620L-1-75620L-10.

[116] Wilmink, G.J., Grundt, J.L., Cerna, C., Roth, C.C., Kuipers, M.A., Lipscomb, D., Echchgadda, I. and Ibey, B.L. (2011) Terahertz Radiation Preferentially Activates the Expression of Genes Responsible for the Regulation of Plasma Membrane Properties. *International Conference on Infrared*, *Millimeter*, *and Terahertz Waves*, Houston, 2-7 October 2011, 1-3. https://doi.org/10.1109/irmmw-THz.2011.6104966

[117] Umezawa, H. (1993) Advanced Field Theory: Micro, Macro, and Thermal Physics. AIP, New York.

[118] Vitiello, G., Radu, C.M., Romano, P., Polcari, A., Iliceto, S., Simioni, P. and Tona, F. (2021) *International Journal of Molecular Sciences*, **22**, Article 156. https://doi.org/10.3390/ijms22010156

[119] Marburgher, J.H. (1975) *Progress in Quantum Electronics*, **4**, 35-110. https://doi.org/10.1016/0079-6727(75)90003-8

[120] Chiao, R.Y., Gustafson, T.K. and Kelley, P.L. (2009) Self-Focusing of Optical Beams. In: Boyd, R.W., Lukishova, S.G. and Shen, Y.R., Eds., *Self Focusing*: *Past and Present*, Springer, New York, 129-143. https://doi.org/10.1007/978-0-387-34727-1_4

[121] Zakharov, V.E. and Shabat, A.B. (1971) *Soviet Journal of Experimental and Theoretical Physics*, **61**, 118-134.

[122] Del Giudice, E., Doglia, S., Milani, M. and Vitiello, G. (1986) *Nuclear Physics B*, **275**, 185-199. https://doi.org/10.1016/0550-3213(86)90595-X

[123] Del Giudice, E., Doglia, S., Milani, M. and Vitiello, G. (1988) Structure, Correlations and Electromagnetic Interactions in Living Matter: Theory and Applications. In: Fröhlich, H., Ed., *Biological Coherence and Response to External Stimuli*, Springer-Verlag, Berlin, 49-64. https://doi.org/10.1007/978-3-642-73309-3_3

[124] Schmieke, M. (2021) *Dev Sanskriti*: *Interdisciplinary International Journal*, **18**, 10-33. https://doi.org/10.36018/dsiij.v18i.226

[125] Salari, V., Tuszynski, J., Rahnama, M. and Bernroider, G. (2011) *Journal of Physics*:

Conference Series, **306**, Article ID: 012075.
https://doi.org/10.1088/1742-6596/306/1/012075

[126] Funk, R.H.W. (2022) *Frontiers in Bioscience*, **14**, Article No. 29.
https://doi.org/10.31083/j.fbe1404029

[127] Pang, X.F. and Chen, X.R. (2001) *Communications in Theoretical Physics* (*Beijing, China*), **35**, 323-326. https://doi.org/10.1088/0253-6102/35/3/323

[128] Pang, X.F., Chen, S., Wang, X. and Zhong, L. (2016) *International Journal of Molecular Sciences*, **17**, Article 1130. https://doi.org/10.3390/ijms17081130

[129] Wong, K.W. and Wan, K.C. (2020) *Journal of Modern Physics*, **11**, 1058-1074,
https://www.scirp.org/journal/jmp
https://doi.org/10.4236/jmp.2020.117067

[130] Spoerke, E.D., Boal, A.K., Bachand, G.D. and Bunker, B.C. (2013) *ACS Nano*, **7**, 2012-2019. https://doi.org/10.1021/nn303998k

[131] Gonzalez, L., De Santis Puzzonia, M., Ricci, R., Aureli, F., Guarguaglini, G., Cubadda, F., Leyn, L., Cundari, E. and Kirsch-Volders, M. (2014) *Nanotoxicology*, **9**, 729-736.
https://doi.org/10.3109/17435390.2014.969791

[132] Geesink, J.H. (2021) Infrared Signal Technology to Make Non-Thermal Non-Ionizing Electromagnetic Waves.

[133] Barlow, P.W. (2015) *Communicative & Integrative Biology*, **8**, e1041696.
https://doi.org/10.1080/19420889.2015.1041696

[134] Palalle, G., Perera, T., Appadoo, D.R.T., Cheeseman, S., Wandiyanto, J.V., Linklater, D., Dekiwadia, C., Truong, V.K., Tobin, M.J., Vongsvivut, J., Bazaka, O., Bazaka, K., Croft, R.J., Crawford, R.J. and Ivanova, E.P. (2019) *Cancer*, **11**, Article No. 162.
https://doi.org/10.3390/cancers11020162

[135] Romanenko, S., Appadoo, D., Lawler, N., Hodgetts, S.I., Harvey, A.R. and Wallace, V.P. (2020) Terahertz Radiation Stimulates Neurite Growth in PC12 Derived Neurons During Development Phase: Preliminary Study. 2020 45*th International Conference on Infrared, Millimeter, and Terahertz Waves* (*IRMMW-THz*), Buffalo, 8-13 November 2020, 1-2. https://doi.org/10.1109/IRMMW-THz46771.2020.9370420

[136] Hough, C.M., Purschke, D.N., Clayton, B., Kalra, A.P., Olivia, P.J., Huang, C., Tuszynski, J.A., Warkentin, B.J. and Hegmann, F.A. (2021) *Biomedical Optics Express*, **12**, 5812-5828. https://doi.org/10.1364/BOE.433240

[137] Tachizaki, T., Sakaguchi, R., Terada, S., Kamei, K.I. and Hirori, H. (2020) *Optics Letters*, **45**, 6078-6081. https://doi.org/10.1364/OL.402815

[138] Romanenko, S., Harvey, A.R., Hool, L. and Wallace, V.P. (2021) *Ex Vivo* Effect of 60 GHz MMW Radiation on Leech Neuron Intracellular Calcium Alteration. 2020 *IEEE Ukrainian Microwave Week* (*UkrMW*), Kharkiv, 21-25 September 2020, 612-616.
https://www.researchgate.net/publication/346882968
https://doi.org/10.1109/UkrMW49653.2020.9252579

Appendix 1. Calculated Coherent and Regulating Frequency Patterns of Microtubules

Nr) Person(s), date: (Applied or measured frequency in Hz, coherent frequency according to algorithm; difference in %)

1) Mavromatos, N.E. Quantum coherence in (brain) microtubules and efficient energy and information transport (2011):

Mavromatos (2011): (2 MHz; 1.9906; 0.47%)

2a) Satyajit Sahu, Subrata Ghosh, Batu Ghosh, Krishna Aswanid, Kazuto Hirata, Daisuke Fujita and Anirban Bandyopadhyay. Atomic water channel controlling remarkable properties of a single brain microtubule: Correlating single protein to its supramolecular assembly (2013):

Sahu *et al.* (2013): (12 Mhz; 11.86; 1.15%)

Sahu *et al.* (2013): (20 Mhz; 19.88; 0.60%)

Sahu *et al.* (2013): (22 Mhz; 22.37; 1.65%)

Sahu *et al.* (2013): (30 Mhz; 29.83; 0.57%)

Sahu *et al.* (2013): (101 Mhz; 100.66; 0.33%)

Sahu *et al.* (2013): (113 Mhz; 113.24; 0.47%)

Sahu *et al.* (2013): (185 Mhz; 189.8; 2.50%)

Sahu *et al.* (2013): (204 Mhz; 201.33; 1.33%)

2b) Satyajit Sahu, Subrata Ghosh, Daisuke Fujita and Anirban Bandyopadhyay.

Live visualizations of single isolated tubulin protein self-assembly via tunneling current: effect of electromagnetic pumping during spontaneous growth of microtubule (2014):

Sahu *et al.* (2014): (1.000 Mhz; 0.995; 0.47%)

Sahu *et al.* (2014): (2.250 Mhz; 2.21; 1.81%)

Sahu *et al.* (2014): (3.770 Mhz; 3.728; 1.07%)

Sahu *et al.* (2014): (5.0 MHz; 4.97; 0.58%)

Sahu *et al.* (2014): (15.00 MHz; 14.91; 0.58%)

Sahu *et al.* (2014): (20.00 MHz; 19.90; 0.60%)

Sahu *et al.* (2014): (0.5 MHz; 0.498; 0.47%)

The typical measured frequencies of these microtubules comply with to the proposed discrete frequencies, described by the proposed algorithm of coherency.

2c) Saxena, K., Singh, P., Sahoo, P., Sahu, S., Ghosh, S., Ray, K., Fujita, D. and Bandyopadhyay, A. Fractal, scale free electromagnetic resonance of a single brain extracted microtubule (2020):

Saxena *et al.* (2020): (30 Mhz; 29.83; 0.57%)

Saxena *et al.* (2020): (7 Ghz; 6.79; 3.09%)

Saxena *et al.* (2020): (13 Ghz; 12.89; 1.33%)

Saxena *et al.* (2020): (19 Ghz; 19.33; 1.70%)

Saxena *et al.* (2020): (22 Ghz; 21.74; 1.18%)

Saxena *et al.* (2020): (160 Thz; 158.3; 1.70%)

Saxena *et al.* (2020): (250 Thz; 250.2; 0.08%)

3) Rafati, Y., Cantu, J.C., Sedelnikova, A., Tolstykh, G.P., Peralta, X.G., Valdez, C. and Echchgadda, I. Effect of microtubule resonant frequencies on neuronal cells (2020): Recent studies suggest that Microtubules (MTs) and tubulin proteins exhibit resonant frequencies in the Radiofrequency (RF) range. It has been hypothesized that exposing neurons to externally applied RF waves tuned to an intrinsic resonant frequency of MTs or tubulin could disrupt the natural signalling occurring in and around them, leading to neurophysiological changes. To test this hypothesis, we assembled custom exposure systems that allow stable RF exposures of cell cultures in a controlled environment (37˚C, 5% CO_2, 95% humidity). Differentiated NG108-15 neuronal cells have been exposed to RF waves tuned to selected resonance peaks for tubulin (91 MHz and 281 MHz) and for MTs (3.0 GHz) for 1 hr at a power density of 0.24 mW/cm^2 (SAR = 0.012, 0.087, and 0.53 mW/kg, respectively). The results suggest that exposing neurons to MTs or tubulin resonant frequencies might affect MTs normal behavior, leading to neurophysiological changes:

Rafati *et al.* (2020): (91 Mhz; 89.5; 1.69%)

Rafati *et al.* (2020): (281 Mhz; 282.8; 0.64%)

Rafati *et al.* (2020): (3.0 GHz; 3.037; 1.22%)

The typical measured frequencies of these microtubules comply with to the proposed discrete frequencies, described by the proposed algorithm of coherency.

4) Koch, M.D., Schneider, N., Nick, P. and Rohrbach, A. Single microtubules and small networks become significantly stiffer on short time scales upon mechanical stimulation (2017):

Koch *et al.* (2017): (0.6 Hz; 0.593; 1.17%)

Koch *et al.* (2017): (1.8 Hz; 1.78; 1.11%)

Koch *et al.* (2017): (2.0 Hz; 2.00; 0%)

Koch *et al.* (2017): (3.0 Hz; 3.0; 0%)

Koch *et al.* (2017): (3.3 Hz; 3.37; 2.08%)

Koch *et al.* (2017): (3.9 Hz; 4.0; 2.50%)

Koch *et al.* (2017): (4.4 Hz; 4.5; 2.22%)

Koch *et al.* (2017): (5.3 Hz; 5.33; 0.57%)

Koch *et al.* (2017): (7 Hz; 7.111; 1.56%)

Koch *et al.* (2017): (11 Hz; 11.31; 2.66%)

Koch *et al.* (2017): (50 Hz; 50.57; 1.69%)

Koch *et al.* (2017): (75 Hz; 75.85; 1.12%)

Koch *et al.* (2017): (100 Hz; 101.14; 1.69%)

Koch *et al.* (2017): (810 Hz; 809.11; 0.109%)

The typical measured coherent frequencies of these microtubules comply with to the proposed discrete frequencies, described by the proposed algorithm of coherency.

5) Pizzi, R., Strini, G., Fiorentini, S., Pappalardo, V. and Pregnolato, M. Evidence of new biophysical properties of microtubules (2010):

Pizzi *et al.* (2010): (1.51 Ghz; 1.519; 0.56%)

6) Li, S., Wang, C. and Nithiarasu, P. Electromechanical vibration of micro-

tubules and its application in biosensor (2019):

Si Li *et al*. (2019): (53.019 MHz; 53.026; 0.01%)

Si Li *et al*. (2019): (159.291 MHz; 159.07; 0.14%)

Si Li *et al*. (2019): (377.840 MHz; 379.62; 0.47%)

Si Li *et al*. (2019): (585.639 MHz; 603.96; 3.03%) (non-circular)

The typical measured coherent frequencies of these microtubules comply with to the proposed discrete frequencies, described by the proposed algorithm of coherency.

7) Barlow, P.W. The natural history of consciousness, and the question of whether plants are conscious, in relation to the Hameroff-Penrose quantum-physical "Orch OR" theory of universal consciousness (2015):

Barlow *et al*. (2015): (40 Hz; 40.50; 1.24%)

8) Palalle, G., Perera, T., Appadoo, D.R.T., Cheeseman, S., Wandiyanto, J.V., Linklater, D., Dekiwadia, C., Truong, V.K., Tobin, M.J., Vongsvivut, J., Bazaka, O., Bazaka, K., Croft, R.J., Crawford, R.J. and Ivanova, E.P. PC 12 heochromocytoma cell response to super high frequency terahertz radiation from synchrotron source (2019):

PC 12 cells were exposed to THz radiation at frequencies ranging from 0.3 to 19.5 THz generated using a synchrotron light source for a period of 10 min. During the THz radiation exposure, the average temperature of the sample was recorded as 25.24˚C ± 0.37˚C. PC 12 cell lines are derived from a pheochromocytoma of the rat adrenal medulla, a mixture of neuroblastic cells and eosinophilic cell. The effect of THz radiation exposure on PC 12 cell differentiation was further investigated by treating the PC 12 cells with NGF and monitoring the neurite outgrowth for up to 7 days. THz-treated PC 12 cells underwent neuronal differentiation, with 86.17% ± 4.06% of the population extending neurites from 0 - 20 μm in length, while 14.90% ± 4.88% of the cell population extended neurites of 20 - 40 μm in length.

9) Romanenko, S., Appadoo, D., Lawler, N., Hodgetts, S.I., Harvey, A.R. and Wallace, V.P. (2020) Terahertz radiation stimulates neurite growth in pc12 derived neurons during development phase: preliminary study (2020):

It was demonstrated that Terahertz (THz) radiation was used as a broadband frequency source to expose neuronal cultures and stimulate intracellular perturbation in cytoskeleton structure and facilitates elongation of tubulin microtubules and actin microfilaments. The phenomenon could have an impact on living cells, especially in the phase of cell development when structural changes in cytoskeleton occur. In this study, the THz/Far-IR Beamline of Australian Synchrotron was used as a broadband source of THz radiation to stimulate perturbation in cytoskeleton structure in neuronal culture. Preliminary results indicate alterations of neurite shape and length in THz exposed cell cultures.

10) Chafai, D.E., Sulimenko, V., Havelka, D., Kubínová, L., Dráber, P. and Cifra, M. (2019) Reversible and irreversible modulation of tubulin self-assembly by intense nanosecond pulsed electric fields:

Tubulin self-assembly into microtubules is a natural phenomenon. Its importance is not just crucial for functional and structural biological processes, but it also serves as an inspiration for synthetic nanomaterial innovations. This work reports a versatile and vigorous strategy for controlling tubulin self-assembly by nanosecond Electropulses (nsEPs). The polymerization assessed by turbidimetry is dependent on nsEPs dosage. It is suggested that changes in C-terminal modification states alter tubulin polymerization-competent conformations. Although the assembled tubulin preserves their integral structure, they might exhibit a broad range of new properties important for their functions. (Remark Geesink: pulses of 11 ns duration fired at 1 Hz are coherent according to the proposed equation of coherence).

11) Hameroff, S.R., Craddock, T.J.A. and Tuszynski, J.A. Quantum effects in the understanding of consciousness (2014):

Conventional neuronal-level computational approaches suggest conscious experience\emerges at a critical level of complexity. Binding is proposed to be accounted for by temporal synchrony (e.g. coherent 40 Hz oscillations).

12) Dotta, B.T., Vares, D.A.E., Buckner, C.A., Lafrenie, R.M. and Persinger, M.A. Magnetic field configurations corresponding to electric field patterns that evoke long-term potentiation shift power spectra of light emissions from microtubules from non-neural cells (2014):

Dotta *et al.* (2014): (9.4 Hz; 9.4816; 0.86%)

Dotta *et al.* (2014): (7.1 Hz; 7.1111; 0.16%)

Dotta *et al.* (2014): (23 Hz; 22.63; 1.65%)

13) Kalra, A.P., Benny, A., Travis, S.M., Zizzi, E.A., Morales-Sanchez, A., Oblinsky, D.G., Craddock, T J.A., Hameroff, S.R., MacIver, M.B., Tuszyński, J.A., Petry, S., Penrose, R. and Scholes, G.D. Electronic energy migration in microtubules (2022):

Kalra *et al.* (2022): (335 nm; 337; 0.59%)

Appendix 2. Calculated Decoherent and Deregulating Frequency Patterns of Microtubules

Nr) Persons, date: (Applied or measured frequency in Hz, decoherent frequency according to algorithm; difference in %)

1) Hough, C.M., Purschke, D.N., Clayton, B., Kalra, A.P., Olivia, P.J., Huang, C., Tuszynski, J.A., Warkentin, B.J. and Hegmann, F.A. Disassembly of microtubules by intense terahertz pulses (2021):

Hough *et al.* (2021): (0.5 THz, 0.505 THz; 0.99%)

Hough *et al.* (2021): (1.5 THz, 1.511 THz; 0.73%)

The typical measured coherent frequencies of these microtubules comply with to the proposed discrete frequencies, described by the proposed algorithm of decoherence.

2) Hintzsche, H., Jastrow C. and Kleine-Ostmann, T. Terahertz radiation induces spindle disturbances in human-hamster hybrid cells (2011):

Hintzsche *et al.* (2011): (0.106 THz; 0.10584; 0.15%)

The typical measured coherent frequencies of these microtubules comply with to the proposed discrete frequencies, described by the proposed algorithm of decoherence.

3) Cantero, M.D.R., Etchegoyen, C.V., Perez, P.L., Scarinci, N. and Cantiello, H.F. (2018) Bundles of brain microtubules generate electrical oscillations (2015):

Cantero *et al.* (2015): (39 Hz; 39.21; 0.54%)

4) Tuszynski, J.A. and Costa, F. Low-energy amplitude modulated radiofrequency electromagnetic fields as a systemic treatment for cancer: Review and proposed mechanisms of action (2022):

Tuszynski and Costa (2012): (27.12 MHz; 27.42; 1.07%)

Appendix 3. Calculated Regulating and Coherent Oscillations of DNA, Stem Cells, Genes, and Proteins

Nr) Persons, date: (Applied or measured frequency in Hz, coherent frequency according to algorithm; difference in %)

1) Nardecchia, I., Torres, J., Lechelon, M.J., Varani, L., Donato, I., Gori, M. and Pettini, M. (2017) Out-of-equilibrium collective oscillations of a model protein in the THz frequency domain (2017):

Nardecchia *et al.* (2017): (0.314 Thz; 0.309; 1.53%)

The typical measured frequencies comply precisely with to the proposed discrete frequencies, described by the proposed algorithm of coherency.

2) Tang, M., Huang, Q., We, D., Zha, G., Chang, T., Ko, K., Wang, M., Du, C., Fu, W. and Cui, H.L. Terahertz spectroscopy of oligonucleotides in aqueous solutions (2015):

Measured coherent EM THz-frequencies, Terahertz spectroscopy of oligonucleotides:

1) 410 GHz
2) 622 GHz
3) 703 GHz
4) 908 GHz
5) 1.38 THz
6) 1.64 THz
7) 1.88 THz
8) 2.08 THz
9) 2.14 THz
10) 2.25 THz
11) 2.55 THz
12) 1.29 THz
13) 1.97 Thz
14) 2.20 THz
15) 2.32 THz
16) 2.47 THz

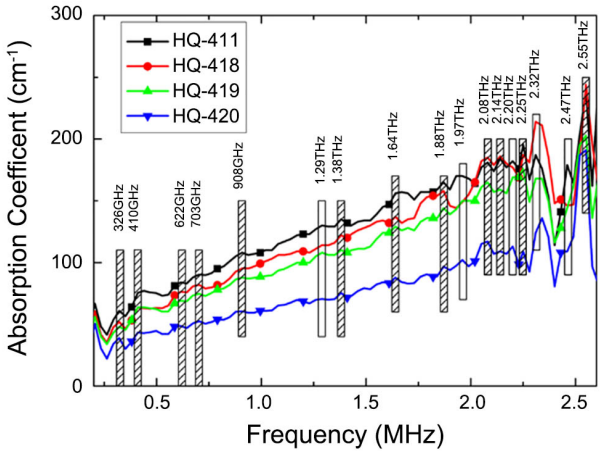

Figure A1. THz absorption spectra of oligo-nucleotide samples. Blank and patterned bars with a width of 30 GHz (spectral resolution) are depicted, respectively indicating similar and different absorption peaks of the four oligonucleotide samples, (reference: Mingjie Tang *et al.*, 2015).

The typical measured coherent frequencies of the oligonucleotides comply with to the proposed discrete frequencies, described by the proposed algorithm of coherency.

3) Titova, L.V., Ayesheshim, A.K., Golubov, A., Rodriguez-Juarez, R., Kovalchuk, A., Hegmann, F.A. and Kovalchuk, O. Intense picosecond THz pulses alter gene expression in human skin tissue *in vivo* (2013):

Titova, L.V., Ayesheshim, A.K., Golubov, A., Rodriguez-Juarez, R., Kovalchuk, A., Hegmann, F.A. and Kovalchuk, O. Intense THz pulses cause H2AX phosphorylation and activate DNA damage response in human skin tissue (2013):

Titova, L.V., Ayesheshim, A.K., Golubov, A., Rodriguez-Juarez, R., Kovalchuk, A., Hegmann, F.A. and Kovalchuk, O. Intense THz pulses down-regulate genes associated with skin cancer and psoriasis: a new therapeutic avenue (2013):

Estimated peaks:

Titova *et al.* (2013): (0.55 THz; 0.55; 0%)

Titova *et al.* (2013): (1.25 THz; 1.237; 1.05%)

Titova *et al.* (2013): (1.84 THz; 1.855; 0.81%)

Titova *et al.* (2013): (1.95 THz; 1.955; 0.25%)

Titova *et al.* (2013): (2.30 THz; 2.32; 0.87%)

Titova *et al.* (2013): (400 nm; 399.5; 0.13%)

At power densities 5.7 and 57 mW/cm^2. The applied Thz frequencies by Titova fit with the proposed quantum equation of coherence.

4) Bogomazova, A.N., Vassina, E.M., Goryachkovskaya, T.M., Popik, V.M., Sokolov, A.S., Kolchanov, N.A., Lagarkova, M.A., Kiselev, S.L. and Peltek, S.E. No DNA damage response and negligible genome-wide transcriptional changes in human embryonic stem cells exposed to terahertz radiation (2015):

Bogomazova *et al.* (2015): (2.3 Thz; 2.317; 0.72%)

The measured frequency of stem cells, related to regulation/ordering fit with

the proposed quantum equation of coherence.

5) Zhao, J., Hu, E., Shang, S., Wu, D., Li, P., Zhang, P., Tan, D. and Lu, X. Study of the effects of 3.1 THz radiation on the expression of recombinant red fluorescent protein (RFP) in *E. coli* (2020):

Zhao *et al.* (2020): (3.1 Thz; 3.11; delta 0.32%)

The applied frequency of 3.1 Thz shows an ordering effect and precisely fit with the proposed quantum equation of coherence.

6) Lechelon, M., Meriguet, Y., Gori, M., Ruffenach, S., Nardecchia, I., Floriani, E., Coquillat, D., Teppe, F., Mailfert, S., Marguet, D., Ferrier, P., Varani, L., Sturgis, J., Torres, J. and Pettini, M. Experimental evidence for long-distance electrodynamic intermolecular force (2022):

Lechelon *et al.* (2021): (71.4 GHz; 72.397; 1.38%)

Lechelon *et al.* (2021); 96 GHz; 97.18; 1.22%)

Both measured frequencies show an ordering effect that fits with the proposed quantum equation of coherence.

7) Hernández-Bule, M.L., Trillo, A.M., Martínez-García, A., Abilahoud, C. and Úbeda, A. (2017) Chondrogenic differentiation of adipose-derived stem cells by radiofrequency electric stimulation (2017):

Hernández-Bule *et al.* (2017): (0.448 MHz; 0.4424; 1.27%)

The applied frequency of 448 KHz shows an ordering effect and precisely fit with the proposed quantum equation of coherence.

8) Safavi, A.S., Sendera, A., Haghighipour, N. and Banas-Zabczyk, A. The role of low-frequency electromagnetic fields on mesenchymal stem cells differentiation: a systematic review (2022).

Appendix 4. Calculated Deregulating and Decoherent Oscillations of DNA, Stem Cells, Genes, and Proteins

Nr) Persons, date: (Applied or measured frequency in Hz, decoherent frequency of algorithm; difference in %)

1a) Lundholm, I.V., Rodilla, H., Wahlgren, W.Y., Duelli, A., Bourenkov, G., Vukusic, J., Friedman, R., Stake, J., Schneider, T. and Katona, J. Terahertz radiation induces non-thermal structural changes associated with Fröhlich condensation in a protein crystal (2015):

1b) Ahlberg Gagnér, A., Lundholm, V.I., Garcia-Bonete, M.J., Rodilla, H., Friedman, R., Zhaunerchyk, V., Bourenkov, G., Schneider, T., Stake, J. and Katon, G. (2019) Clustering of atomic displacement parameters in bovine trypsin reveals a distributed lattice of atoms with shared chemical properties (2019):

Ahlberg Gagnér *et al.* (2019): (0.5 THz, 0.505 THz; 0.99%)

2a) Alexandrov, B.S., Rasmussen, K.O., Bishop, A.R., Usheva, A., Alexandrov, L.B., Chong, S., Dagon, Y., Booshehri, L.G., Mielke, C.H., Phipps, M.L., Martinez, J.S., Chen, H.T. and Rodriguez, G. Non-thermal effects of terahertz radiation on gene expression in mouse stem cells (2011):

2b) Alexandrov, B.S., Phipps, M.L., Alexandrov, L.B., Booshehri, L.G., Erat, A., Zabolotny, J., Mielke, C.H., Chen, H.T., Rodriguez, G., Rasmussen, K.O., Marti-

nez, J.S., Bishop, A.R. and Usheva, A. Specificity and heterogeneity of terahertz radiation effect on gene expression in mouse mesenchymal stem cells (2013):

Alexandrov *et al.* (2011): (2.52 THz; 2.54; 0.78%)

Alexandrov *et al.* (2013): (2.52 THz; 2.54; 0.78%)

Alexandrov *et al.* (2013): (10.0 THz; 10.16; 1.60%)

The typical measured frequencies comply with to the proposed discrete frequencies, described by the proposed algorithm of decoherence.

3) Bock, J., Fukuyo, Y., Kang, S., Phipps, M.L., Alexandrov, L.B., Rasmussen, K.O., Bishop, A.R. Rosen, E.D., Martinez, J.S., Chen, H.T., Rodriguez, G., Alexandrov, B.S. and Usheva, A. Mammalian stem cells reprogramming in response to terahertz radiation (2010):

Bock *et al.* (2010): (10.0 THz; 10.16; 1.60%)

Average density power 1 mW/cm^2, broadband THz radiation (10 THz) at a high repetition rate (1 kHz). The typical measured frequencies comply with to the proposed discrete frequencies, described by the proposed algorithm of decoherence.

4a) Echchgadda, I., Grundt, J.E., Cerna, C.Z., Roth, C.C., Ibey, B.L. and Wilmink, G.J. Terahertz stimulate specific signaling pathways in human cells, in 39th International Conference on Infrared, Millimeter, and Terahertz Waves (2014):

4b) Echchgadda, I., Cerna, C.Z., Sloan, M.A., Elam, D.P. and Ibey, B.L. Effects of different terahertz frequencies on gene expression in human keratinocytes (2015):

4c) Echchgadda I., *et al.* Terahertz radiation: a non-contact tool for the selective stimulation of biological responses in human cells (2016):

4) Echchgadda *et al.* (2014, 2015): (2.52 THz; 2.54; 0.79%)

Exposure at 44.2 mW/cm^2. The typical measured frequencies comply with to the proposed discrete frequencies, described by the proposed algorithm of decoherence.

5a) Wilmink, G.J., Rivest, B.D., Roth, C.C., Ibey, B.L., Payne, J.A., Cundin, l.X., Grundt, J.E., Peralta, X., Mixon, D.G. and Roach, W.P. *In vitro* investigation of the biological effects associated with human dermal fibroblasts exposed to 2.52-THz radiation (2011):

5b) Wilmink, G.J., Rivest, B.D., Ibey, B.L. Roth, C.C., Bernhard, J. and Roach, W.P. Quantitative investigation of the bioeffects associated with terahertz radiation (2010):

5c) Wilmink, G.J., Grundt, J.L., Cerna, C., Roth, C.C., Kuipers, M.A., Lipscomb, D., Echchgadda, I. and Ibey, B.L. Terahertz radiation preferentially activates the expression of genes responsible for the regulation of plasma membrane properties (2011):

5d) Grundt, J.E., Cerna, C., Roth, C.C., Ibey, B.L., Lipscomb, D., Echchgadda, I. and Wilmink, G.J. Terahertz radiation triggers a signature gene expression profile in human cells (2011):

Wilmink *et al.* (2010, 2011, 2014): (2.52 THz; 2.54; 0.79%)

84.8 mW/cm^2 and 227 mW/cm^2. The typical measured frequencies comply with to the proposed discrete frequencies, described by the proposed algorithm of decoherence.

6) Tachizaki, T., Sakaguchi, R., Terada, S., Kamei, K.I. and Hirori, H. Terahertz pulse-altered gene networks in human induced pluripotent stem cells (2020):

An apparatus has been developed for studying the effects of THz pulse irradiation on living human induced pluripotent stem cells. The THz pulse, 0.8 THZ, of the maximum electric field reached 0.5 MV/cm and was applied for one hour with 1 kHz repetition to the entire cell-culture area, a diameter of 1 mm. RNA sequencing of global gene-expression revealed that many THz-regulated genes were driven by zinc-finger transcription factors. Combined with a consideration of the interactions of metal ions and a THz electric field, these results imply that the local intracellular concentration of metal ions, such as Zn2+, was changed by the effective electrical force of our THz pulse. (Remark Geesink: probably disrupting).

Tachizaki *et al.* (2010): (0.8 THz; 0.8011; 0.137%)

7) Sergii Romanenko, Alan R. Harvey, Livia Hool, Vincent P. Wallace. Ex Vivo Effect of 60 GHz MMW radiation on Leech Neuron Intracellular Calcium Alteration (2021). https://www.researchgate.net/publication/346882968:

Opposite to conductive heating alterations in neuronal electrophysiological activity was reported. This induces the question regarding the intracellular calcium homeostasis in neurons, due to critical importance of intracellular level of free calcium for neuron's activity. This study at 60 GHz, indicated upregulation of free intracellular calcium in ex vivo experiment along with corelating morphological changes in the leech ganglia neuron.

Appendix 5. Quantum Informational Code: Calculated Examples of Coherent Frequencies from Sub-Hertz Till PHz

Factor	F1,m	F2,m	F3,m	F4,m	F5,m	F6,m	F7,m	F8,m	F9,m	F10,m	F11,m	F12,m
m = 0 (Hz)	1.0000	1.0535	1.1250	1.1852	1.2656	1.3333	1.4142	1.5000	1.5803	1.6875	1.7778	1.8984
m = 2^1 (Hz)	2.0000	2.1070	2.2500	2.3704	2.5312	2.6666	2.8284	3.0000	3.1606	3.3750	3.5556	3.7968
m = 2^2 (Hz)	4.0000	4.2140	4.5000	4.7408	5.0624	5.3332	5.6568	6.0000	6.3212	6.7500	7.1112	7.5936
m = 2^5 (Hz)	32.000	33.712	36.000	37.9264	40.499	42.665	45.254	48.000	50.569	54.000	56.889	60.748
m = 2^8 (Hz)	256.00	269.70	288.00	303.41	324.00	341.33	362.04	384.00	404.54	432.00	455.12	486.00
m = 2^{12} (KHz)	4.0960	4.3151	4.6080	4.8546	5.1839	5.4613	5.7926	6.1440	6.4729	6.9120	7.2819	7.7759
m = 2^{24} (MHz)	16.777	17.675	18.874	19.884	21.233	22.370	23.726	25.166	26.513	28.312	29.827	31.850
m = 2^{32} (GHz)	4.2950	4.5248	4.8318	5.0904	5.4357	5.7266	6.0739	6.4425	6.7873	7.2478	7.6356	8.1536
m = 2^{40} (THz)	1.0995	1.1583	1.2370	1.3031	1.3915	1.4660	1.5549	1.6493	1.7376	1.8554	1.9547	2.0873
M = 2^{48} (THz)	281.47	296.53	316.66	333.60	356.23	375.29	398.06	422.21	444.81	474.99	500.41	534.35
Colors												
Color wavelength (nm)	532.5	505.6	473.4	449.3	420.8	399.5	376.6	710.1	674.0	631.3	599.1	561.0

Appendix 6. Analyses and a Fit of Measured Normalized Microtubule Frequencies Described by Proposed Quantum Equation of Coherence

Table A1. Derived normalized eigenfrequencies of microtubules by multiplying or dividing by 2^n, (n is an integer) and positioned in a normalized invariant MHz-scale ("black numbers" are coherent/organizing/healthy states; "red or bold numbers" are decoherent/disorganizing/unhealthy states). First row (bold): eigenstates of proposed algorithm in MHz.

Algorithm Mhz >> 16.777	**17.675**	**18.874**	**19.884**	***20.548***	**21.233**	**22.370**	***23.038***	**23.726**	***24.436***	**25.166**	***25.831***	**26.513**	***27.398***	**28.312**	**29.827**	***30.822***	**31.850**
K16.7	S18	S19	S20	***C20.5***	B21.0	S22	***H22.9***	R23.4	***Ta24.5***	S25.3	***H25.9***	S26	***T27.1***	S28.3	S30	***H30.5***	M32
K16.4	R17.6	K18.5	S20		S21.48	R22.8		S24		S25.5		L26.5		S28	S30.2		S31.3
		S19.2	S20		Ha21.0	K22.2		P23.6		k25.2		K26.2		K27.7	S30		S31.3
			L19.9		Bh21.0			S23.1		D24.8		K26.2			S30		S32
			K20.1					L23.6				K26.5			K30.1		
			K19.7					K23.7				Ka26.4			K29.4		
			D19.7												D29.8		

References of authors: S: Sahu and Saxena; R: Rafati; P: Pizzi; L: li; K: Koch; C: Cantero; B: Barlow; Bh: Bhamerof; H: Hough; h: Hintzsche; T: Tuszynski; Ta: Tachizaki; Ha: Hameroff; D: Dotta; Ka: Kalra.

Appendix 7

Energy distribution of Bose-Einstein condensates and Bosons

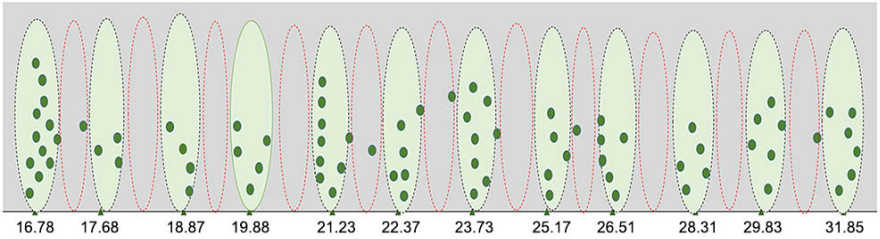

Normalized frequencies (MHz) and Numbers of informational quantum code

Figure A2. Normalized frequency data of Bose-Einstein condensate and Boson peak experiments (1995-2020) positioned in a coherent toroidal scale of frequencies. Exposures at frequencies are in the bands of Hz, Khz, MHz, GHz, PHz. Green triangles plotted on a logarithmic x-axis represent normalized coherent frequencies in MHz; green points represent calculated normalized Bose-Einstein condensate and Boson-peak frequencies. For clarity, points are distributed along the Y-axis. **Literature references:** Bose-Einstein condensate and Boson peak experiments (1995-2020): Dzyapko *et al.* (2007), Nguyen *et al.* (2019), Klaers *et al.* (2010), Griesmaier *et al.* (2008), Weber et al. (2003), Davis *et al.* (1993), Weill *et al.* (2019), Cabrera-Gutiérrez *et al.* (2019), Borisenko *et al.* (2020), Chen *et al.* (2019), Tikhomirov *et al.* (2001), Richet (2012), Nakayama (2002), Schroeder (2004), Aubin (2005), Martin (1999), Chang (2006), Lauber (2011), Surendran (2015), Zhang (2020), Lucioni (2019), Anderson (1995), Brennecke (2008), Vasudev (2016), Hau (2009).